Volume 12
Number 7
July 2020
Pages 1011–1172

# Metallomics

Integrated biometal science

rsc.li/metallomics

ISSN 1756-591X

ROYAL SOCIETY OF CHEMISTRY

**PAPER**
Deborah A. Roess, Debbie C. Crans *et al.*
Polyoxometalates function as indirect activators of a G protein-coupled receptor

Indexed in Medline!

Metallomics

PAPER

View Article Online
View Journal | View Issue



Cite this: *Metallomics*, 2020, **12**, 1044

# Polyoxometalates function as indirect activators of a G protein-coupled receptor†

Duaa Althumairy,[ab] Kahoana Postal,[cd] B. George Barisas,[ac] Giovana G. Nunes,[d] Deborah A. Roess*[ae] and Debbie C. Crans*[ac]

Received 22nd February 2020,
Accepted 18th May 2020

DOI: 10.1039/d0mt00044b

rsc.li/metallomics



The luteinizing hormone receptor (LHR), a G protein-coupled receptor (GPCRs), can initiate signaling in the presence of some vanadium-containing compounds as a result of vanadium compound interactions with the membrane lipids and/or the cell membrane lipid interface. The ability of LHR expressed in CHO cells to initiate signaling in the presence of highly charged and water-soluble polyoxovanadates (POV) including $Na_3[H_3V_{10}O_{28}]$ (**$V_{10}$**) and two mixed-valence heteropolyoxovanadates, $K(NH_4)_4[H_6V_{14}O_{38}(PO_4)]\cdot 11H_2O$ (**$V_{14}$**) and $[(CH_3)_4N]_6[V_{15}O_{36}(Cl)]$ (**$V_{15}$**), was investigated here. Interactions of the vanadium compounds with CHO cells decreased the packing of membrane lipids, drove aggregation of LHR and increased signal transduction by LHR. Cell responses were comparable to, or in the case of **$V_{14}$** and **$V_{15}$**, greater than those seen for cells treated with human chorionic gonadotropin (hCG), a naturally-occurring LHR ligand produced in early pregnancy in humans. POV effects were observed for CHO cells where LHR was expressed at 10 000 or 32 000 LHR per cell but not when LHR was overexpressed with receptor numbers >100 000 LHR per cell. To determine which POV species were present in the cell medium during cell studies, the speciation of vanadate (**$V_1$**), **$V_{10}$**, **$V_{14}$** or **$V_{15}$** in cell medium was monitored using $^{51}V$ NMR and EPR spectroscopies. We found that all the POVs initiated signaling, but **$V_{15}$** and **$V_{10}$** had the greatest effects on cell function, while **$V_1$** was significantly less active. However, because of the complex nature of vanadium compounds speciation, the effects on cell function may be due to vanadium species formed in the cell medium over time.

**Significance to metallomics**

The following manuscript describes initiation of signal transduction of the luteinizing hormone receptor induced by vanadate and polyoxovanadates. Polyoxovanadates are generally large hydrophilic water-soluble anions that are not compatible with the hydrophobic lipid environments. Regardless, decavanadate was reported to initiate signal transduction by the plasma membrane insulin receptor. It is not known whether POVs have similar effects on other membrane proteins functioning as G protein-coupled receptors. This manuscript describes the initiation of signal transduction by the plasma membrane luteinizing hormone receptor by these polyoxometalates and demonstrate that highly charged vanadium anions are also able to initiate signal transduction.

## Introduction

Polyoxometalates (POM) belong to a large diverse class of anionic materials that exhibit a wide range of chemical and physical properties.[1–6] They are often salts with highly charged inorganic anions and both organic and inorganic cations. Polyoxovanadates (POVs) are a subgroup of POMs containing vanadium oxides. Mixed-valence POV compounds (MV-POV) expand the observed chemistry of this class by specifically supporting redox chemistry that may also facilitate a wider range of biological effects. POMs are known to interact with proteins functioning as enzyme inhibitors[7–14] and to facilitate protein crystallization[15–18] as well as having other functions relevant to disease processes.[4,5,19–22] The compounds have been considered as potential treatments for diseases such as AIDS, cancer, and diabetes.[3,19,23,24] POMs are reported to interact with ribosomes, as demonstrated by X-ray structure,[15–17] and with acid phosphatase A.[25,26] In some systems, the POM interaction is

[a] *Cell and Molecular Biology Program, Colorado State University, Fort Collins, CO 80523, USA. E-mail: Debbie.Crans@colostate.edu*
[b] *Department of Biological Sciences, King Faisal University, Saudi Arabia*
[c] *Department of Chemistry, Colorado State University, Fort Collins, CO 80523, USA*
[d] *Department of Chemistry, Universidade Federal do Paraná, Curitiba, Paraná, 81.531-980, Brazil*
[e] *Department of Biomedical Sciences, Colorado State University, Fort Collins, CO 80523, USA*

† Electronic supplementary information (ESI) available: Time-dependent $^{51}V$ NMR and EPR spectra of aqueous solutions are included. See DOI: 10.1039/d0mt00044b

very favorable as is the case for the activated tyrosine kinase receptor, pdb code 3gqi.[25,26] This receptor, although treated with vanadate, contained a bound decavanadate in its X-ray structure.[25] Although some POMs have been found to penetrate cells,[3] POMs, because of their large structures, are generally believed to exert their mode of action from the outside of the cell.[27] POMs may also affect chemical reactions mediated by proteins in biological systems *via* indirect interactions with other eukaryotic cell components.[28–31]

To examine biological effects of POVs on intact cells and, more specifically membrane proteins involved in transduction of extracellular signals to the cell interior, we evaluated cellular responses of the luteinizing hormone receptor (LHR), a member of the G protein-coupled receptor family.[32] G protein-coupled receptors are a superfamily of more than almost 1000 receptors, that mediate responses to light, odors, hormones, and neurotransmitters and transmit a signal to the cell interior. These receptors make up approximately 40% of drug targets.[33] LHR, members of the subgroup of G protein-coupled receptors that bind a glycoprotein ligand, are involved in reproductive function in both males and females.[34] They are structurally related to rhodopsin, a G protein-coupled receptor for which a crystal structure together with an associated G protein is available[35] and to the more structurally complex β-adrenergic receptor.[36] As is the case for follicle stimulating hormone receptors, for which detailed structural information is available,[37] binding of a glycoprotein hormone at the LHR's extracellular binding site initiates transduction of signal across the plasma membrane where intracellular receptor structures activate G proteins and intracellular signaling cascades.[34] As part of hormone-mediated signaling, LHR translocate to cholesterol-rich plasma membrane microdomains[38,39] where locally high concentrations of LHR result in aggregation of these receptors and initiation of signal transduction to the cell cytoplasm.[40]

Here we describe time-dependent, indirect effects of a series of POV complexes on LHR. Important to these studies, cell lines are available that stably express human LHR at low, physiologic numbers, approximately 10 000–32 000 LHR per cell, as well as over-express the receptor which leads to receptor crowding and constitutive receptor aggregation.[41] We have previously shown that treatment of cells expressing physiologically relevant numbers of LHR with a known antidiabetic vanadium compound, bismaltolatooxovanadium(IV) (abbreviated BMOV with a formula $[H_{10}V^{IV}C_{12}O_7]$), or a vanadium(IV) salt, vanadyl sulfate, $V^{IV}OSO_4$, can like a hormone induce extensive clustering of receptor dimers resulting in signal transduction by LHR.[41] When receptor density is low, LHR receptor aggregation occurs in response to BMOV or $VOSO_4$, both of which interact with the plasma membrane lipid bilayer. Signaling by the LHR receptor appears to occur as a result of the indirect effects of BMOV or $VOSO_4$ on membrane lipid packing. However, since the effects of BMOV and $VOSO_4$ are different,[41] this documents the fact that the speciation matters in this system as well as others differ as has been reported previously.[42,43] It is therefore important to carry out speciation analysis under the conditions of the GPCR studies in this system in order to properly interpret the effects of the compounds.[43,44]

POVs can be homopolyoxovanadates with only vanadium-oxides or heteropolyoxovanadates in which vanadium oxides are combined with other elements. The anions consist of $VO_4$ tetrahedral or $VO_6$ octahedral components to generate small oligomers and the compact decavanadate ($[V_{10}O_{28}]^{6-}$, abbreviated as $\mathbf{V_{10}}$). MV-POVs, in turn, generally combine V(IV) and V(V) metal ions in $VO_5$ square-pyramidal units to generate structures that differ from $\mathbf{V_{10}}$ and affect the POVs chemistry. Specifically, we investigated both classes of POVs including $[Na_2(H_2O)_{10}]\,[H_3V^{V}_{10}O_{28}\{Na(H_2O)_2\}]\cdot 3H_2O$ ($\mathbf{V_{10}}$), $K(NH_4)_4[H_6V^{IV}_2V^{V}_{12}O_{38}(PO_4)]\cdot 11H_2O$ ($\mathbf{V_{14}}$) and $[(CH_3)_4N]_6\,[V^{IV}_7V^{V}_8O_{36}(Cl)]$ ($\mathbf{V_{15}}$). Importantly, $\mathbf{V_{10}}$ contains 10 V(V) atoms with $Na^+$ counterions, while $\mathbf{V_{14}}$ contains 12 V(V) and 2 V(IV) atoms with $K^+$ and $NH_4^+$ counterions with an encapsulated phosphate, and $\mathbf{V_{15}}$ contains 7 V(V) and 8 V(IV) atoms with 6 $(CH_3)_4N^+$ cations with an encapsulated chloride. The structures of the POVs used in this paper are shown schematically in Fig. 1.

Unlike vanadium compounds such as BMOV or other organic vanadium-compounds, POVs are generally highly charged anions and, as a result, water-soluble and often lipid-insoluble. Studies in

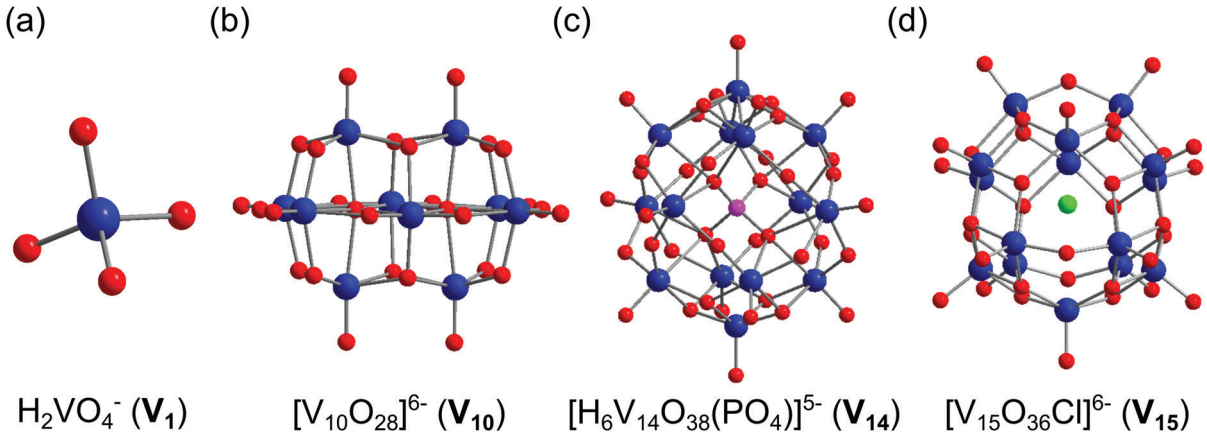


Fig. 1 Ball and stick representation of anions: metavanadate ($\mathbf{V_1}$), decavanadate ($\mathbf{V_{10}}$), phosphotetradecavanadate ($\mathbf{V_{14}}$) and chloropentadecavanadate ($\mathbf{V_{15}}$). The hydrogen atoms are omitted for clarity. Vanadium atoms are blue, oxygen is red, phosphate is pink, and chloride is green.

model membrane systems, such as microemulsions, also referred to as reverse micelles, have been reported.[45,46] In studies involving $\mathbf{V_{10}}$ materials, properties change with the cation although the $\mathbf{V_{10}}$ anion remains in the middle of the water droplet and does not interact directly with the interface of the nanosized micelle. We anticipate that the repulsion of the negatively charged surfactant at the interface with the highly negative charged (six minus) $\mathbf{V_{10}}$ anion is affecting the placement of the anion far from the interface.[45,46] However, the nature of the $\mathbf{V_{10}}$ interactions with the interface varies with changes in the cation, affecting the solubility of the different $\mathbf{V_{10}}$ materials in microemulsions.[47–49] Specifically, the low solubility observed for the sodium salt of $\mathbf{V_{10}}$ is increased 2–3 times with the metforminium salt.[49] We attribute these differences to the interactions of the metforminium counterions, which penetrate the negatively charged interface of the reverse micelle. Interactions of $\mathbf{V_1}$ and other oligomeric anions with the interface have also been reported and, for these small oxovanadates, the changes observed in the oxovanadate species chemical shifts and their concentration is interpreted to suggest that these species are located at the interface of the reverse micelle.[50,51]

There are several reasons for interest in these compounds and their effects on cell function. First, most of the vanadium compounds investigated previously have been able to interact strongly with the interface or to penetrate the interface.[45,47–49] $\mathbf{V_{10}}$ and other water-soluble POMs are located in the aqueous phase in model systems[46,50,52] and this presumably limits their interactions with hydrophobic lipid molecules in cell membranes. Although $\mathbf{V_{10}}$ is able to initiate signaling by insulin receptors, it is not known whether POVs have similar effects on other membrane proteins functioning as endocrine hormone receptors. $\mathbf{V_{14}}$ and $\mathbf{V_{15}}$ are of interest in this regard because of their partial structural similarity with $\mathbf{V_{10}}$. However, because they are mixed-valence POMs, their chemistry is more complex. $\mathbf{V_{15}}$ is more stable compared to $\mathbf{V_{14}}$ which undergoes speciation in aqueous solution, representing compounds with very different properties and the potential for ROS formation and/or consumption, which have been invoked in the action of several POMs effects in biological systems.[23,27,53,54] Finally, POV speciation in cell medium must be measured under the conditions that promote cell growth inhibition because species arising from the parent compounds may be important for biological activity.

To determine whether a series of POMs affected plasma membrane lipid packing and aggregation of LHR, we evaluated time-dependent changes in lipid packing following treatment of CHO cells with $\mathbf{V_1}$, $\mathbf{V_{10}}$, $\mathbf{V_{14}}$, or $\mathbf{V_{15}}$, as well as the aggregation state and activity of LHR in CHO cells expressing the receptor. The major question addressed in this work is whether classes of highly charged vanadium-containing POMs that are water-soluble promote aggregation of LHR and receptor-mediated signaling. These studies also examined if the indirect effects of the POMs on membrane lipids persist in cells after removing the POMs from the cell medium. Persistence of membrane effects due to POMs reflects high-affinity interactions of these compounds with membrane lipids, charge interactions with the membrane's extracellular matrix or, perhaps, internalization. These results suggest a need for further investigation of these compounds and their mode of action. A time course of effects on cells and characterization of speciation chemistry in cell culture medium provided here establish the species present during activation of LHR signal transduction initiation.

## Materials and methods

### Materials

The Chinese Hamster Ovary (CHO) cell line, CHO-K1, was kindly provided by Dr Takamitsu Kato at Colorado State University. Dulbecco's Modified Eagle medium (DMEM) and geneticin were purchased from Corning Cellgro. Penicillin/streptomycin and L-glutamine solution were purchased from Gemini Bio-Products (West Sacramento, CA). Fetal bovine serum (FBS) was purchased from Atlas Biologicals (Fort Collins, CO). 100× MEM non-essential amino acid solution, bovine albumin, and $NaVO_3$ were purchased from Sigma-Aldrich (St. Louis, MO). $\mathbf{V_{10}}$ ($[Na_2(H_2O)_{10}][H_3V_{10}O_{28}\{Na(H_2O)_2\}]\cdot 3H_2O$)[55,56] or [$\{Na_6(H_2O)_{20}V_{10}O_{28}\cdot 4H_2O\}_n$],[55,56] $\mathbf{V_{14}}$ ($K(NH_4)_4[H_6V_{14}O_{38}(PO_4)]\cdot 11H_2O$)[53] and $\mathbf{V_{15}}$ ($[[(CH_3)_4N]_6[V_{15}O_{36}(Cl)]]$)[57] were prepared as described previously. Trypsin–EDTA (0.25%) was purchased from Fisher Scientific Co (Pittsburgh, PA). Optimal-MEM was purchased from Life Technologies (Carlsbad, CA), CA35 mm diameter glass-bottom cell culture dishes were purchased from In Vitro Scientific (Sunnyvale, CA).

### Stock solutions of $\mathbf{V_1}$, $\mathbf{V_{10}}$, $\mathbf{V_{14}}$ and $\mathbf{V_{15}}$

The 10 mM stock solutions of $\mathbf{V_1}$, $\mathbf{V_{10}}$, $\mathbf{V_{14}}$, and $\mathbf{V_{15}}$ were freshly prepared by dissolving the compounds in water and then adding phosphate-buffered saline (PBS), pH 7.3, containing 1.0 mM $CaCl_2$ and 0.50 mM $MgCl_2$. For homo-transfer fluorescence resonance energy transfer (homo-FRET) studies to assess LHR aggregation or assays of cAMP, dilutions of $\mathbf{V_1}$, $\mathbf{V_{10}}$, $\mathbf{V_{14}}$ or $\mathbf{V_{15}}$ stock solutions were made into serum-free media (500 mL of DMEM, 5.0 mL of 100× non-essential amino acid solution, 5.0 mL of penicillin/streptomycin and 5.0 mL of L-glutamine solution) to obtain cell media containing the POVs at final concentrations obtained from cell viability studies described below (10 μM for $\mathbf{V_1}$, 2.0 μM for $\mathbf{V_{10}}$, 4.0 μM for $\mathbf{V_{14}}$ and 6.0 μM for $\mathbf{V_{15}}$). Media containing POVs were prepared immediately before beginning cell studies.

### Assessing the $IC_{50}$ for $\mathbf{V_1}$, $\mathbf{V_{10}}$, $\mathbf{V_{14}}$, and $\mathbf{V_{15}}$ in cell viability assays

To verify the effects of the vanadium compounds on CHO cell growth and to select appropriate concentrations of these compounds for further cell studies, growth inhibition assays were carried on using resazurin-based fluorometric assay and serial dilutions of $\mathbf{V_1}$, $\mathbf{V_{10}}$, $\mathbf{V_{14}}$, and $\mathbf{V_{15}}$ stock solutions into DMEM cell media. This cell viability assay effectively counts the number of viable cells in a fixed volume of cell media. Approximately 20 000 cells per well were seeded in 96-well plates in 100 μl serum free media and allowed to attach for 3 h. Cells were then treated with 1.0, 5.0, 10, 50 or 100 μM of $\mathbf{V_1}$, $\mathbf{V_{10}}$, $\mathbf{V_{14}}$ or $\mathbf{V_{15}}$ together with 10% resazurin for 3 h to obtain a baseline value for the number of cells. This was designated as time 0. A separate

 

population of cells was similarly treated with each compound for 12 h before the addition of 10% resazurin for an additional 3 h ($t$ = 15 h). After the incubation with resazurin, fluorescence measurements at time 0 and after 15 h were made to assess cell number. An excitation wavelength of 530 nm was used with the measurement of emission at 590 nm. To establish control rates of cell growth, the estimated number of live cells at time 0 and the estimated number of cells after exposure to **$V_1$**, **$V_{10}$**, **$V_{14}$**, and **$V_{15}$** at $t$ = 15 h were expressed as a ratio of values at $t$ = 15/$t$ = 0 and expressed as a percentage of control cell numbers for untreated CHO cells. Inhibitory concentrations at which 50% of cells died ($IC_{50}$) for CHO cells treated with **$V_1$**, **$V_{10}$**, **$V_{14}$** or **$V_{15}$** were calculated by fitting curves to log values for each vanadium compound. Values shown are the average of triplicate responses from three separate experiments using nonlinear regression with three parameters. Results were graphed using GraphPad Prism 8. The concentrations of **$V_1$**, **$V_{10}$**, **$V_{14}$** or **$V_{15}$** used in subsequent cell experiments were less than or approximately equal to the $IC_{25}$ values for each compound (Table 1). These concentrations were efficacious without causing high levels of cell death over the time course of cell studies.

### $V_1$, $V_{10}$ or $V_{15}$ effects on membrane lipid order

These studies used an environmentally sensitive styryl dye, di-4-ANEPPDHQ, to evaluate the extent of lipid packing in the cell membrane. Membranes containing a high fraction of lipids with double bonds in their fatty acids tend to be more disordered. Reducing the number of double bonds in membrane phospholipids or adding cholesterol to the membrane tends to increase lipid packing. The fluorescent dye used in these studies, di-4-ANEPPDHQ, was tested initially in model membranes where it demonstrated an approximately 60 nm shift in fluorescence emission when the lipid used formed a more disordered, *i.e.* less densely packed, membrane at 20 °C. A mixture of cholesterol and dipalmitoyl-phosphocholine produced a more ordered membrane and increased dye emission at 570 nm. The technique that we use depends on evaluating the emission ratio at 620 nm and 535 nm and looking for shifts in the emission ratio with cell treatment. This is a well-established method[58–61] and one that we have used previously in studies using vanadium or chromium compounds to treat viable cells.[28,29,41]

To evaluate the effects of POVs on membrane lipid order, untransfected CHO cells were grown to 80–90% confluence in 25 $cm^2$ culture flasks and then incubated with 1.0 mL trypsin–EDTA (0.25%) for 3 min. Cells (0.5 mL) were seeded into six 35 mm glass-bottom Petri dish. After 12 h, cells were washed twice with 1× PBS (pH 7.3) then incubated in medium containing either **$V_1$**, **$V_{10}$** or **$V_{15}$**. One dish was immediately labeled with 200 μL of 1.5 μM di-4-ANEPPDHQ stock solution for 15 min, washed and immersed in a 1× PBS buffer for imaging using a Zeiss Axiovert 200M inverted microscope.[41] The remaining dishes were incubated with **$V_1$**, **$V_{10}$**, or **$V_{15}$** in media for 10 h. At the indicated times, dishes were removed from the incubator, cells were washed once, resuspended in medium free serum and imaged at time 0, 1, 2, 6, and 24 h after labeling with di-4-ANEPPDHQ using a Zeiss Axiovert 200 M inverted microscope equipped with a 63 × 1.2 NA water objective and an Andor Du897E EMCCD camera. Cell samples were illuminated with an arc lamp with a 480/30× or 495/20× excitation filter. Fluorescence emission was collected simultaneously in channel 1 using a 535/40 nm filter and in channel 2 using a 620/40 nm filter. MetaFluor software was used to observe and image cells during experiments. Background correction for each image and fluorescence intensity ratio of 620 nm/535 nm calculations were performed using Image J. In some experiments examining effects of **$V_1$** or **$V_{15}$** on membrane lipid order, cells at $t$ = 0 and 6 h were washed two additional times (designated 2× and 3×) prior to measurements of membrane lipid order. The goal of these experiments was to assess the degree of association of **$V_1$** or **$V_{15}$** with the cell membrane.

### Polarized homo-fluorescence resonance energy transfer measurements

The extent of LHR aggregation was evaluated using polarized homo-transfer fluorescence resonance energy transfer (homo-FRET) methods and performed as previously described using CHO cell lines expressing either 10 000, 32 000, 122 000 or 560 000 LHR per cell in their plasma membranes.[41] These human LHR were tagged on their intracellular C-terminus with a covalently linked enhanced yellow fluorescence protein to provide a fluorescence signal (hLHR-eYFP).[41] FRET between hLHR-eYFP occurs to a significant extent when donor eYFP and acceptor eYFP moieties attached to LHR on its intracellular domain are within 2–10 nm of each other.[62] Under those conditions, polarized excitation of one YFP molecule leads to energy transfer and non-polarized emission by the second YFP molecule. The degree of polarized emission is a measure of the relative number of molecules in close proximity to

Table 1 Calculated values for the $IC_{50}$ in Chinese Hampster Ovary (CHO) cells treated with **$V_1$**, **$V_{10}$**, **$V_{14}$**, and **$V_{15}$**

| V-Compound | $IC_{50}$ per V-compound (μM) | $IC_{50}$ per vanadium atom[a] (μM) | $IC_{25}$ per V-compound (μM) | Selected concentration for each V-compound based on $IC_{25}$[b] (μM) |
|---|---|---|---|---|
| **$V_1$** | 56.5 ± 7.5 | 56.5 ± 7.5 | 20.0 | 10.0 |
| **$V_{10}$** | 3.2 ± 0.6 | 32 ± 6.0 | 1.6 | 2.0 |
| **$V_{14}$** | 6.1 ± 0.8 | 84 ± 11 | 3.4 | 4.0 |
| **$V_{15}$** | 8.2 ± 3.2 | 123 ± 48 | 5.5 | 6.0 |

[a] This column shows the concentration of vanadium atoms in the form of the indicated compound needed to produce the observed $IC_{50}$. [b] The concentration selected for use in cell studies was less than or approximately equal to the compound's $IC_{25}$ to minimize cell death over the time course of the experiment while maintaining efficacy.

one another as has been described for microscope- and flow cytometer-based applications.[63–65]

Briefly, cells were grown to 80–90% confluence in 25 cm culture flasks in DMEM medium and then incubated with 1.0 mL trypsin–EDTA (0.25%) for 3 min. Cells (0.5 mL) were plated in 35 mm glass-bottom Petri dishes. After 12 h, the cells were washed twice with 1× phosphate buffer, saline (PBS; pH 7.3) and then treated for 10 h with either 10 μM **V$_1$**, 2.0 μM **V$_{10}$**, 4.0 μM **V$_{14}$** or 6.0 μM **V$_{15}$**. Cells were then washed once to remove the vanadium compounds, resuspended in serum-free medium and imaged using homo-FRET methods immediately ($t = 0$) or after 1, 2, 3, 6 or 24 h. Homo-FRET images were collected using a Zeiss Axiovert 200 M inverted microscope with an Andor Du897E EMCCD camera and MetaMorph software. Arc lamp illumination passing through a vertically-polarized filter provided polarized excitation. Approximately 16 images were acquired at a rate of one image per min with a 15 s exposure time. This exposure typically bleaches the eYFP tag covalently attached to the C-terminus of the LHR to ∼10% of its initial fluorescence intensity. A Princeton Instruments Dual View image splitter created side-by-side images of fluorescence polarized parallel or perpendicular to the excitation polarization. Backgrounds were subtracted from fluorescence emission images and a *g*-factor was calculated to correct for efficiency differences in instrument optics as previously described.[66] The *g*-factor constitutes the instrument-specific correction for different detection sensitivities for vertically- and horizontally-polarized fluorescence. The intrinsic anisotropy of a single eYFP fluorophore is 0.38.[66] About 5–7 cells were examined from each Petri dish and at least 30 cells were examined for each treatment. We assumed monomeric LHR tagged with eYFP exhibited this value and set to 0.38 the apparent anisotropy upon complete bleaching. Homo-FRET results were expressed as mean ± SEM. Statistical evaluation of mean differences in untreated and treatment groups was analyzed by one-way ANOVA followed by the Tukey multiple comparison test and Student's *t*-test to compare between two groups using R version 3.3.1. $P$ values $< 0.05$ were considered statistically significant.

### Measurements of intracellular cAMP levels using the ICUE3 reporter

Fluorescence assays of intracellular cyclic adenosine monophosphate (cAMP) were made using a cAMP reporter ICUE3 expressed in CHO cells from an ICUE3 plasmid provided by Dr Jin Zhang.[67] ICUE3 has a single cyclic nucleotide-binding domain and is based on the Epac probe, Epac1 149–881. It is fused to an enhanced cyan fluorescent protein (CFP) and a circularly-permuted Venus cpV-L194.[67] In the absence of cAMP, the probe is folded with CFP close to the Venus eYFP which gives rise to substantial energy transfer from CFP to eYFP and sensitized emission from eYFP. cAMP binding unfolds the probe, reducing FRET and causing an accompanying increase in CFP emission and a decrease in eYFP sensitized emission. After transfection of CHO cells with the ICUE3 plasmid, images were acquired with PBS to establish baseline levels of intracellular cAMP. Then the cell media was exchanged with solutions containing 100 nM hCG, 10 μM **V$_1$**, 2.0 μM **V$_{10}$**, 4.0 μM **V$_{14}$** or 6.0 μM **V$_{15}$** for 15 min. Both before and after cell treatment, images were acquired used a 63 × 1.2 NA water objective in a Zeiss Axiovert 200M inverted microscope with an Andor Du897E EMCCD camera, arc lamp excitation with a 436DF20 excitation filter and two emission filters, 480DF40 for CFP and 535DF30, for eYFP and eYFP sensitized emission (YFPSE) due to energy transfer from CFP. All filters were from Chroma Technology. Images were acquired at 60 s intervals using MetaFluor software. After background subtraction from fluorescence images, data were analyzed using Image J software to calculate the emission intensity ratios CFP/YFPSE. For each Petri dish, 2–5 cells were observed, and data were collected from at least 15 cells for each treatment.

### Spectroscopic investigation of vanadium species

The nature of the V-species in solution was determined using both vanadium nuclear magnetic resonance ($^{51}$V NMR) and electron paramagnetic resonance (EPR) spectroscopy. These analyses are non-trivial for two reasons; soluble vanadium(v) species exchange rapidly[68] in contrast to the much slower exchanging POVs,[69] and because biological studies are done in complex buffers[43,44] where conversion between oxidation states of the vanadium can occur.[70–73] Our experiments and analysis are based on a vast literature of vanadium speciation chemistry which included studies elucidating the different vanadium(v) species[74–77] as well as vanadium(iv) species,[74,78–81] and support the assignments of the known species we see as hydrolysis products. **V$_1$** and **V$_{10}$**, are compounds with vanadium in oxidation state V(v), while **V$_{14}$** and **V$_{15}$** are mixed-valence POVs and present both V(v) and V(iv) in their compositions. However, under the conditions used in cell studies, the vanadium oxidation state can undergo redox chemistry to form a mixture of vanadium(v) and (iv) complexes. It is therefore important that the vanadium(iv) species are monitored using EPR spectroscopy and the vanadium(v) species are monitored using $^{51}$V NMR spectroscopy. **V$_1$**, **V$_{10}$**, **V$_{14}$**, and **V$_{15}$** samples were prepared at 1.0 mM concentrations in serum-free media as described below for both $^{51}$V NMR and EPR analyses.

In the $^{51}$V NMR studies, solutions containing **V$_1$** and the polyoxovanadates, **V$_{10}$**, **V$_{14}$**, and **V$_{15}$**, were used to characterize the vanadium(v) species formed in DMEM media. Spectra were recorded at ambient temperature using a Bruker spectrometer at 78.9 MHz for $^{51}$V and 400.13 MHz for $^{1}$H. The $^{51}$V NMR spectra were recorded at several time-points (0, 3, 10, 24 h) to determine whether there were changes in the speciation during a 24 h interval. The parameters used for the $^{51}$V NMR studies were similar to those reported previously.[41,82] $^{51}$V NMR spectra for the **V$_1$**, **V$_{10}$**, **V$_{14}$**, and **V$_{15}$** samples were recorded using an external reference of $Na_3VO_4$ (100 mM, pH 12.8, signals at −535 (**V$_1$**) and −559 ppm ($V_2$)) and the values are referenced against $VOCl_3$.[68]

EPR spectroscopy was used to characterize the vanadium(iv) species formed in DMEM media. Spectra were recorded at ambient temperature using a Bruker ESR-300 spectrometer operating in X-band and previously described methods reducing the microwave absorbance of the aqueous solution.[82] The solutions, prepared at 1.0 mM concentrations, were recorded in

 

1 mm glass capillary tubes that were placed in 2 mm quartz tubes. A powder sample of 2,2-diphenyl-1-picrylhydrazyl (DDPH, $g$ = 2.0037) was used as an external standard. The spectra were recorded at 9.84 GHz frequency and 0.6325 mW microwave power with modulation frequency 100.00 kHz, modulation amplitude 10.00 G, time constant 5.12 ms, sweep width 2000.00 G, sweep time 5.24 s, resolution of 2048 points and sixteen scans with a central field at 3511.20 G. The EPR spectra were recorded at 0, 3, 6, 10 and 24 h time points.

## Results

### Concentration-dependent effects of $V_1$, $V_{10}$, $V_{14}$, and $V_{15}$ on cell viability

Initial studies were performed to evaluate concentration dependent effects of **$V_1$**, **$V_{10}$**, **$V_{14}$** or **$V_{15}$** on CHO viability. The goal of these studies was to identify the $IC_{25}$ and $IC_{50}$, *i.e.* the concentrations of vanadium compounds that caused 25% and 50% reduction in cell viability for CHO cells treated with each vanadium compound for times that approximated the incubation time used in measurements of cell function (Table 1). **$V_1$**, **$V_{10}$**, **$V_{14}$**, and **$V_{15}$** decreased CHO cell viability over the 15 h timescale of this experiment, Fig. 2. All $IC_{50}$ concentrations for **$V_1$**, **$V_{10}$**, **$V_{14}$** or **$V_{15}$** were greater than 1.0 μM but less than the $IC_{25}$. It is noteworthy that **$V_{10}$** was most effective in reducing cell viability followed by **$V_{14}$** and **$V_{15}$**. **$V_1$** had the least effect on cell viability in these studies. Concentrations of 10 μM for **$V_1$**, 2.0 μM for **$V_{10}$**, 4.0 μM for **$V_{14}$** and 6.0 μM for **$V_{15}$** were selected for use in subsequent experiments. These concentrations were less than or approximately equal to the $IC_{25}$ for each compound and were concentrations where, under experimental conditions, >75% of cells remained viable over the duration of the experiment.

### Effects of $V_1$, $V_{10}$ or $V_{15}$ on lipid order in CHO cell plasma membranes

Previous studies in selected eukaryotic cell lines have shown that V-compounds capable of interacting strongly with membrane lipids[45,47–49] affect lipid order and, as a result, lipid packing in the cell membranes. Most of the vanadium compounds investigated previously have been able to interact strongly with the interface or penetrate the interface.[45,47–49] Because **$V_{10}$** and other water-soluble POMs are located in the aqueous phase in model systems,[46,50,52] their ability to interact with hydrophobic lipid molecules in cell membranes is presumably limited. Thus, the function of these experiments was to assess whether these water-soluble compounds affected membrane lipid order, a property that appeared important in the function of more hydrophobic vanadium compounds.[29,41] Following a 10 h pre-incubation of CHO cells with **$V_1$**, **$V_{10}$** or **$V_{15}$** lipid packing was decreased when compared to untreated cells as indicated by an increase in the ratio of emission of di-4-ANEPPDHQ at 640/545 nm (Fig. 3a). After washing cells once to remove excess **$V_1$**, **$V_{10}$** or **$V_{15}$** from the cell medium, lipid packing was monitored over 24 h. By 24 h, lipid packing had returned to baseline values suggesting that, under these conditions, **$V_1$**, **$V_{10}$** or **$V_{15}$** effects on membrane lipid order

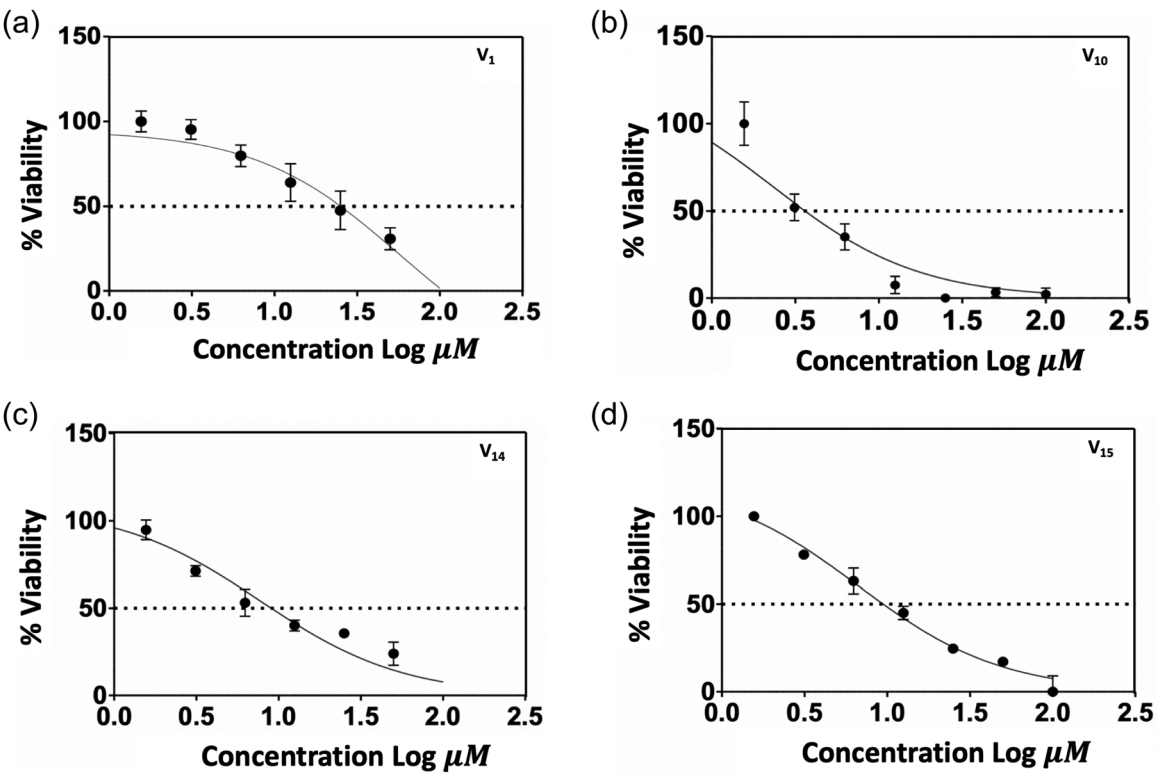


Fig. 2 Effect of **$V_1$** (a), **$V_{10}$** (b), **$V_{14}$** (c), and **$V_{15}$** (d) on CHO cell viability. The dashed line at 50% viability was used to establish the $IC_{50}$ for each of these compounds.

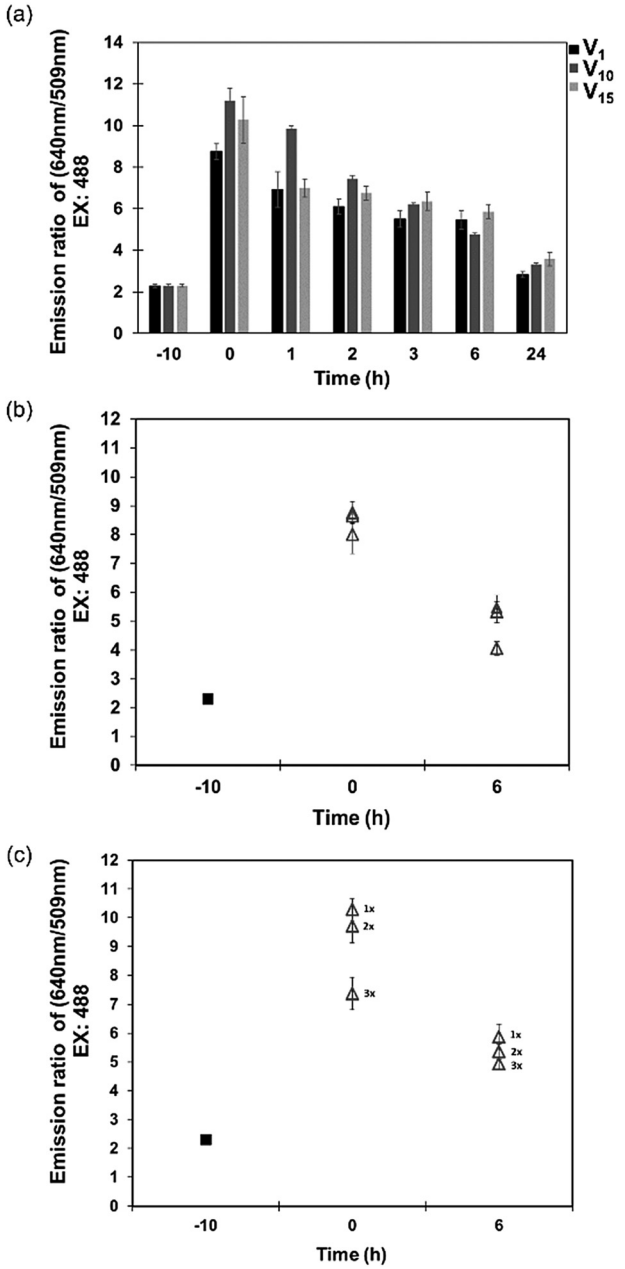


Fig. 3 (a) Membrane lipid order in CHO cells treated with $\mathbf{V_1}$, $\mathbf{V_{10}}$, and $\mathbf{V_{15}}$. Cells were preincubated with $\mathbf{V_1}$, $\mathbf{V_{10}}$ or $\mathbf{V_{15}}$ for 10 h and then washed once to remove the vanadium compounds from the cell medium. The extent of lipid packing as indicated by the emission ratio at 640/545 nm following excitation of the fluorophore with 488 nm light was monitored over 24 h. Increased emission at 640 nm relative to emission at 545 nm is indicative of a decrease in lipid order. In (b) and (c), the effects of repeated washing at time 0 and time 6 h on lipid fluidity for cells was assessed in (b) for $\mathbf{V_1}$ and in (c) for $\mathbf{V_{15}}$. A second and third wash appeared to increase lipid order and is indicated on the graphs by 2× and 3× labels, respectively. No return to the value seen for untreated cells was observed in any of the washed cells.

had decreased steadily over this time. Interestingly, cells treated with $\mathbf{V_1}$, which had the least effect on cell viability when compared to other POVs, exhibited the least effect on lipid packing in these studies. This compound is also the material that is interacting the most with the interphase, based on model studies,[50] and could thus be anticipated to internalize.

To evaluate the extent of $\mathbf{V_1}$ or $\mathbf{V_{15}}$ association with the membrane, cells were washed two additional times at 0 and 6 h before assessing lipid packing in some experiments (Fig. 3b and c, respectively). These studies were not done with $\mathbf{V_{14}}$ because, as shown below, this compound decomposed very rapidly and results would, for this reason, be difficult to interpret meaningfully. Because POVs are not hydrophobic and $\mathbf{V_{10}}$ does not appear to insert in the lipid interface of reverse micelles,[9,46,52] one could anticipate that $\mathbf{V_{15}}$, in particular, would be readily washed from the extracellular surface of the cell. However, neither at time 0 nor time 6 h did additional washings result in a return to baseline values for lipid order suggesting that at least some $\mathbf{V_1}$ or $\mathbf{V_{15}}$ remained tightly associated with the cell membrane, had undergone chemistry with surface proteins or was internalized. Because large POMs with high superficial charges, such as $\mathbf{V_{15}}$, are not readily interacting with hydrophobic interfaces and membranes, this observation would suggest that the effects of these compounds on the membrane fluidity and/or the initiated signaling resulted in some changes that did allow for membrane interaction or internalization of the POV. If membrane proteins underwent conformation changes resulting from interactions with $\mathbf{V_1}$ or $\mathbf{V_{15}}$, this result would be observed although hydrolysis and internalization would be more likely, particularly for $\mathbf{V_1}$.

Effects of $\mathbf{V_1}$, $\mathbf{V_{10}}$, $\mathbf{V_{14}}$ or $\mathbf{V_{15}}$ pretreatment on LHR aggregation were examined using CHO cell lines stably expressing 10 000 LHR, 32 000 LHR, 122 000 LHR or 560 0000 LHR per cell, Fig. 4. When cells expressed 10 000 or 32 000 LHR per cell, preincubation of cells with 10 μM $\mathbf{V_1}$, 2.0 μM $\mathbf{V_{10}}$, 4.0 μM $\mathbf{V_{14}}$ or 6.0 μM $\mathbf{V_{15}}$ produced extensive aggregation of LHR under conditions that also decreased lipid order in CHO cell membranes. Interestingly, $\mathbf{V_{14}}$ and $\mathbf{V_{15}}$ had a greater effect on LHR aggregation than did hCG, the naturally occurring ligand for human LHR which has been, to date, the most effective molecule used to aggregate the receptor. This includes other gonadotropins capable of binding the LHR and other vanadium compounds.[41,83] In contrast to results for cells expressing either 10 000 or 32 000 LHR per cell, overexpression of LHR was associated with constitutive aggregation of the receptors as has been previously observed.[41] For cells expressing 560 000 LHR per cell, there was no further aggregation of LHR when cells were treated with hCG or pre-treated with $\mathbf{V_1}$, $\mathbf{V_{10}}$, $\mathbf{V_{14}}$ or $\mathbf{V_{15}}$ despite the decrease in lipid order caused by $\mathbf{V_1}$ or these POVs.

### Effects of $\mathbf{V_1}$, $\mathbf{V_{10}}$, $\mathbf{V_{14}}$, and $\mathbf{V_{15}}$ on cAMP levels in CHO cells

There appears to be a comparatively simple relationship between receptor clustering as demonstrated in homo-FRET studies of LHR anisotropy and intracellular levels of cAMP, Fig. 5.[41,84] Receptors that are extensively clustered, either from the binding of hCG, exposure of cells to $\mathbf{V_1}$ or POVs, or overexpression of LHR, are also actively signaling. When considering cells expressing 10 000 LHR per cell, this relationship is apparent. Untreated receptors exhibit high values for initial anisotropy and have low basal levels of intracellular cAMP as indicated by the ratio of CFP/YFPSE which is low. Treating cells with either 100 nM

 

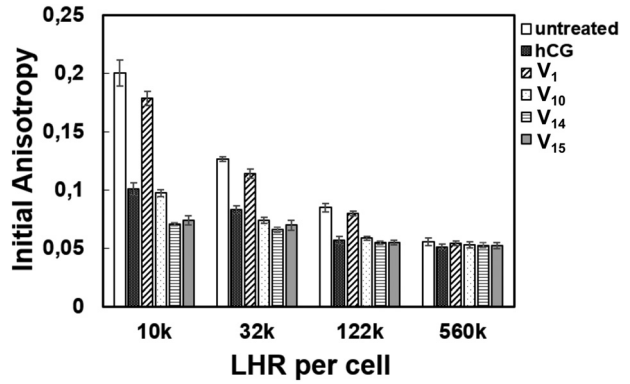


Fig. 4 Values for the initial anisotropy measured for eYFP covalently linked to LHR using polarized homo-FRET methods. Smaller values for initial anisotropy are indicative of LHR aggregation. Pre-treatment of cells with $\mathbf{V_1}$, $\mathbf{V_{10}}$, $\mathbf{V_{14}}$ or $\mathbf{V_{15}}$ decreased values for initial anisotropy for receptors on cells expressing 10 000 or 32 000 LHR per cell. $\mathbf{V_1}$ had less effect on LHR aggregation than did hCG. The effects of $\mathbf{V_{10}}$, $\mathbf{V_{14}}$, and $\mathbf{V_{15}}$ were comparable to hCG or greater than the effect of hCG on LHR aggregation. When cells expressed non-physiologically high numbers of LHR per cell, receptors were extensively aggregated. For cells expressing 122 000 LHR per cell, hCG, $\mathbf{V_{10}}$, $\mathbf{V_{14}}$, and $\mathbf{V_{15}}$ caused a small increase in receptor aggregation while $\mathbf{V_1}$ had no statistically significant effect on receptor clustering. There was no statistically significant effect of hCG, $\mathbf{V_1}$ or POVs on receptor clustering when cells expressed 560 000 LHR per cell suggesting that highly over-expressed LHR are extensively clustered and that receptors are not affected by changes in lipid order.

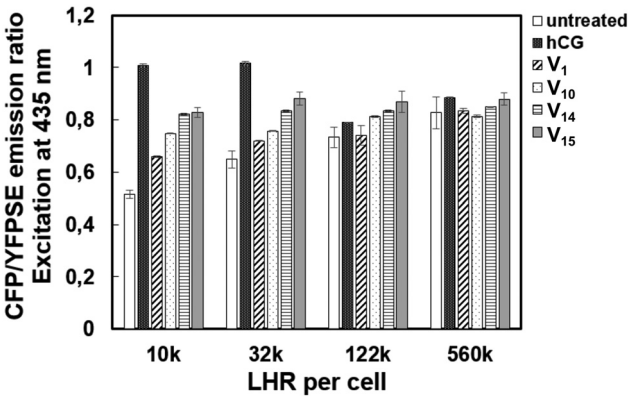


Fig. 5 The effects of LHR numbers per cell on intracellular cAMP levels in the absence (control) or presence of 100 nM hCG or on cells treated with $\mathbf{V_1}$, $\mathbf{V_{10}}$, $\mathbf{V_{14}}$ or $\mathbf{V_{15}}$. ICUE3 was used as a cAMP reporter molecule. When there is an increase in intracellular cAMP, cAMP binds to ICUE3, reduces energy transfer between CFP and YFP (YFPSE) upon exposure of ICUE3 to 435 nM light and increases the CFP/YFPSE ratio. In the absence of cAMP, there is increased energy transfer from CPF to YFP, an increase in sensitized emission by YFP, and a reduction in the CFP/YFPSE ratio. Data shown are the mean and S.E. of 25–43 individual measurements depending on the treatment.

hCG or $\mathbf{V_1}$, $\mathbf{V_{10}}$, $\mathbf{V_{14}}$ or $\mathbf{V_{15}}$ for 15 min increases intracellular cAMP. Exposing CHO cells to these various molecules also causes anisotropy values to decrease, indicating LHR clustering. Basal levels of intracellular cAMP in untreated cells increase with increasing numbers of LHR per cell and these increased levels of cAMP per cell are associated with decreasing initial anisotropies. When cells overexpress LHR, as for example, when cells express 122 000 or 560 000 LHR per cell, the addition of 100 nM hCG, $\mathbf{V_1}$ or POVs has little or no effect on intracellular cAMP levels which are already high. These receptors are pre-clustered and, as a result, constitutively active.

### Monitoring the stability of $\mathbf{V_1}$, $\mathbf{V_{10}}$, $\mathbf{V_{14}}$ or $\mathbf{V_{15}}$ in cell medium

The speciation and stability of $\mathbf{V_1}$, $\mathbf{V_{10}}$, $\mathbf{V_{14}}$ or $\mathbf{V_{15}}$ and the respective oxidation products were monitored in DMEM media since it was not possible to monitor compound stability in the cell membrane (Fig. 6–9). In Fig. 6, the $^{51}$V NMR and EPR spectra of 1.0 mM of $\mathbf{V_1}$ in media are shown. The left panel shows the dissolution of 1.0 mM of $NaVO_3$ which is mainly present as $\mathbf{V_1}$ + VP (where VP corresponds to the phosphate–vanadate complex formed in solution) with some dimeric $H_2V_2O_4^{2-}$ ($V_2$) and tetrameric $V_4O_{12}^{4-}$ ($V_4$) forming at pH 7.4. The right panel shows the EPR spectra observed from the same sample and demonstrates that a very low amount of vanadium(IV) is forming in this solution from the added vanadium(V). This shows that the addition of $\mathbf{V_1}$ to CHO cells does lead to the formation of large amounts of vanadium(IV) species as has previously been reported in yeast.[85] However, over the course of the incubation, the vanadium(IV) signal decreases and, at 24 h, none is observed suggesting that the low level of V(IV) is indeed observed. The reoxidation to vanadium(V), not detectable by EPR, was presumably caused by the oxygen presented in the air and diffusing into the sample.

In Fig. 7 the $^{51}$V NMR and EPR spectra of 1.0 mM of $\mathbf{V_{10}}$ added to the media is shown. These spectra show that the simple oxovanadates form immediately, but that some $\mathbf{V_{10}}$ persist up to about 10 h. In addition, some V(IV) is observed during the period $\mathbf{V_{10}}$ is present in solution, but at 24 h when $\mathbf{V_{10}}$ is no longer present in the media, the amount of V(IV) is also significant reduced.

In Fig. 8, the $^{51}$V NMR and EPR spectra of 1.0 mM of $\mathbf{V_{14}}$ in DMEM media at pH 7.4 is shown. The left panel is showing the $^{51}$V NMR spectra of 1.0 mM of $\mathbf{V_{14}}$ and the speciation is documenting that a little $\mathbf{V_1}$ + PV with trace amounts of $\mathbf{V_{10}}$ is present at the initial hour (0 h). Since the $\mathbf{V_{14}}$ cluster contains 12 V(V) and 2 V(IV) atoms, the $^{51}$V NMR spectrum initially has a low intensity of vanadium(V) signals because the presence of vanadium(IV) atoms in the structure makes the MV-POV compound undetectable by the $^{51}$V NMR spectroscopy. After 3 h of incubation, the concentration of vanadium(V) in solution has increased, $V_2$ and $V_4$ have formed and there is no longer evidence of $\mathbf{V_{10}}$. By 24 h, the $\mathbf{V_{14}}$ sample is likely completely oxidized and hydrolyzed and only the small vanadium(V) oligomers are present. In Fig. 8 (right) the EPR spectra of 1.0 mM of $\mathbf{V_{14}}$ is shown and is consistent with the mixed-valence oxometalate reported previously.[53] The spectrum of the $\mathbf{V_{14}}$ registered at room temperature contains a single line with $g = 1.8999$ and $\Delta_{p-p} = 18$ G, due to the delocalization of the two electrons from the two reduced V-atoms in the $\mathbf{V_{14}}$ structure.[86] The EPR spectrum for the $\mathbf{V_{14}}$ persists beyond the 6 h but is absent at the 10 h time point. The shoulder in the spectrum indicates the formation of a second species, which could be the $\mathbf{V_{14}}$

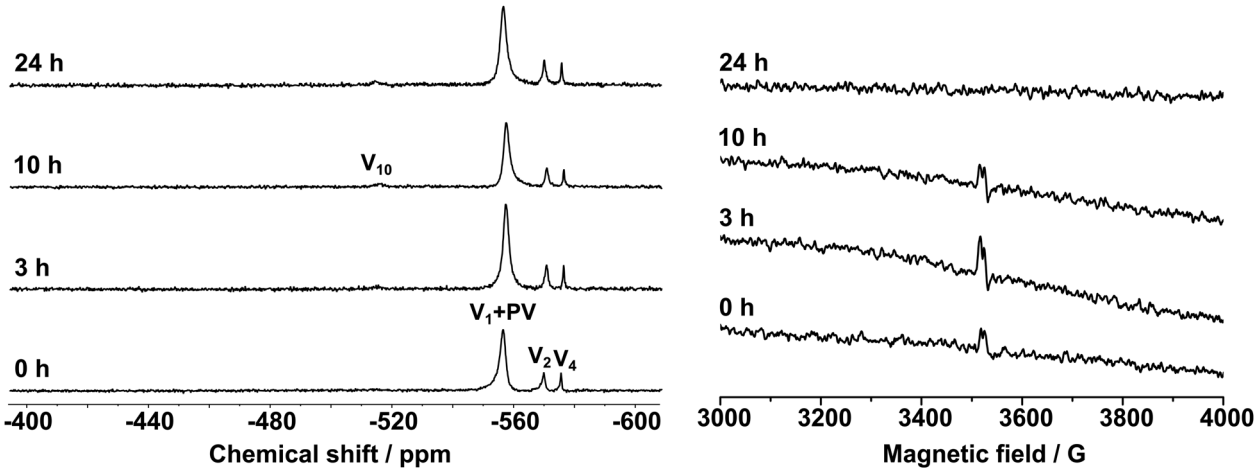


Fig. 6 The $^{51}$V NMR (left) and the EPR spectra (right) are shown as a function of time after the CHO cells have been incubated with 1.0 mM of $NaVO_3$, $\mathbf{V_1}$, for 34 h at pH 7.4. Only one spectrum is shown for the 24 h and 34 h since identical spectra are observed. The observed signals at $\delta$ = −555, −570 and −575 ppm were assigned to $\mathbf{V_1}$ + PV = $H_2VO_4^-$, $V_2$ = $H_2V_2O_7^{2-}$ and $V_4$ = $V_4O_{12}^{4-}$, respectively. The peak at −513 ppm is to the most intense signal of $\mathbf{V_{10}}$ and can sometimes be observed first in spectra where the low concentration of $\mathbf{V_{10}}$ is present.

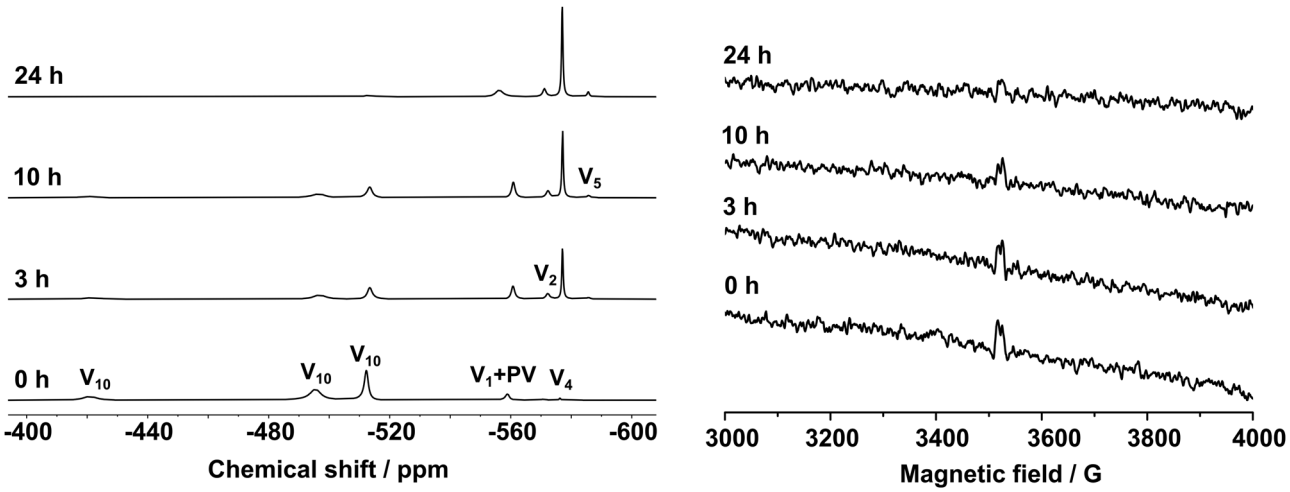


Fig. 7 The $^{51}$V NMR (left) and the EPR spectra (right) are shown as a function of time after the CHO cells have been incubated by 1.0 mM of the sodium decavanadate salt, $\mathbf{V_{10}}$, for 34 h at pH 7.4. Only one spectrum is shown for the 24 and 34 h since identical spectra were observed. The signals with $\delta$ (ppm) are assigned to $\mathbf{V_1}$ + PV = $H_2VO_4^-$ in rapid equilibrium with the VP-complex (−559), $V_2$ = $H_2V_2O_7^{2-}$ (−570), $V_4$ = $V_4O_{12}^{4-}$ (−575), $V_5$ = $V_5O_{15}^{5-}$ (−584) and to the three signals of $\mathbf{V_{10}}$ = $V_{10}O_{28}^{6-}$ (−421, −495 and −511).

containing only one V(IV) or to the aqueous V(IV) mononuclear species. Considering that the *g*-value for the $VOSO_4$ sample,[87] previously reported, is similar to the species observed for the reduced parts in the $\mathbf{V_1}$ sample in media, we conclude that the observed signal can be potentially attributed to a vanadium(IV) formed as an adduct with a component of the media and is not the free vanadyl cation ($VO^{2+}$) in aqueous solution or the partially oxidized POV. This finding is in agreement with previous observations.[53] These spectra suggest that the $\mathbf{V_{14}}$, responsible for the EPR signal, is disappearing and by 10 h is mainly gone. This also shows that the addition of $\mathbf{V_{14}}$ to the CHO cells does result in some interaction of the intact MV-POV for at least 6 h before it has been completely hydrolyzed and oxidized, and no longer observed after 24 h. Combined, these results show that the $\mathbf{V_{14}}$ structure is intact only for the first hour of the experiments and that the vanadium(IV) is oxidized during the incubation and after 24 h there is no V(IV) left to be observed by EPR spectroscopy. Importantly, this means vanadium(IV) is only found at early timepoints in the experiment.

In Fig. 9 the $^{51}$V NMR and EPR spectra of 1.0 mM of $\mathbf{V_{15}}$ in DMEM media are shown. The left panel is showing the $^{51}$V NMR spectra of 1.0 mM $\mathbf{V_{15}}$ and the speciation shows that little $\mathbf{V_1}$ + PV with trace amounts of $V_2$ and $V_4$ is present at pH 7.4 initially (0 h). Since the $\mathbf{V_{15}}$ cluster contains 7 V(V) and 8 V(IV) atoms, the $^{51}$V NMR of this MV-POV will present no signal, as was observed for $\mathbf{V_{14}}$. Intact solutions of $\mathbf{V_{15}}$ will contain low concentrations of vanadium(V) species as seen at initial times. However, after 3 h of incubation, the concentration of vanadium(V) in solution has increased and $\mathbf{V_1}$ + PV, $V_2$, and $V_4$ have formed. No evidence for $\mathbf{V_{10}}$ or oxidized $\mathbf{V_{15}}$ was seen in

 

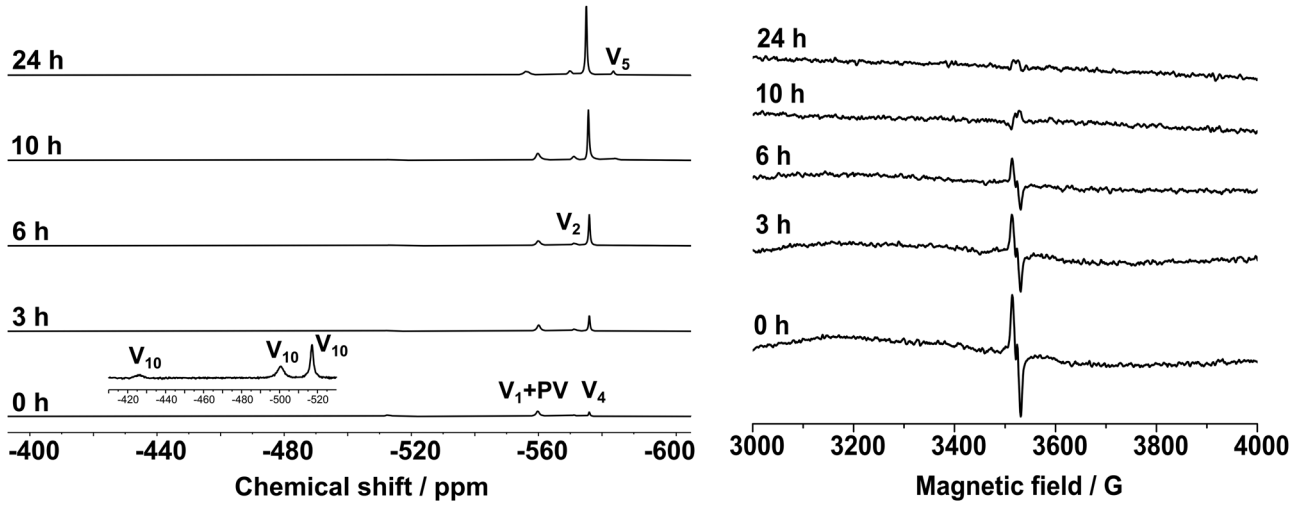


Fig. 8 The $^{51}$V NMR (left) and the EPR spectra (right) are shown as a function of time after the CHO cells have been incubated by 1.0 mM of $K(NH_4)_4[H_6V_{14}O_{38}(PO_4)]\cdot 11H_2O$, **$V_{14}$**, for 34 h at pH 7.4. Only one spectrum is shown for the 24 h and 34 h since identical spectra are observed. The signals with $\delta$ (ppm) are assigned to **$V_1$** + PV = $H_2VO_4^-$ in rapid equilibrium with the VP-complex (−560), $V_2$ = $H_2V_2O_7^{2-}$ (−571), $V_4$ = $V_4O_{12}^{4-}$ (−575), $V_5$ = $V_5O_{15}^{5-}$ (−584) and to the three signals of **$V_{10}$** = $V_{10}O_{28}^{6-}$ (−425, −499 and −516).

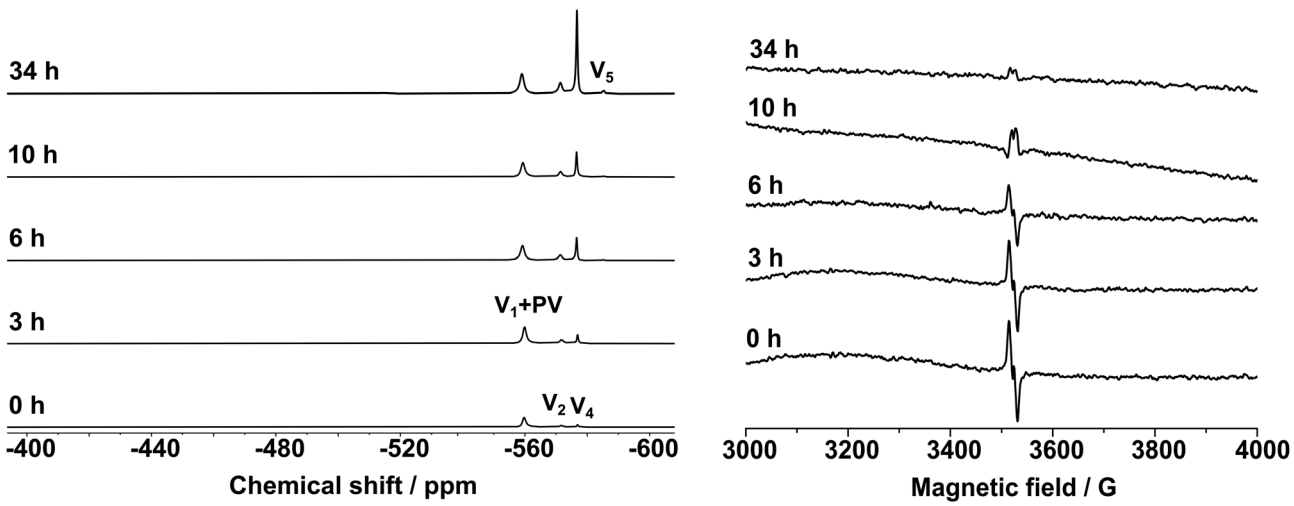


Fig. 9 The $^{51}$V NMR (left) and the EPR spectra (right) are shown as a function of time after the CHO cells have been incubated with 1.0 mM of $[(CH_3)_4N]_6[V_{15}O_{36}(Cl)]$, **$V_{15}$**, for 34 hours at pH 7.4. The signal at −559 ppm was assigned as **$V_1$** + PV = $H_2VO_4^-$ in rapid equilibrium with the VP-complex. And the signals at −570, −575 and −584 ppm were attributed to $V_2$ = $H_2V_2O_7^{2-}$, $V_4$ = $V_4O_{12}^{4-}$, and $V_5$ = $V_5O_{15}^{5-}$, respectively. The speciation observed in these solutions show that **$V_{15}$** is mostly intact at the beginning of the incubation because very little vanadate is observed. Some of the **$V_{15}$** remains intact at the end of the incubation period examined. No evidence for the formation of **$V_{10}$** was observed.

any of these samples. A fully oxidized **$V_{15}$** has been previously described by single-crystal X-ray diffraction and by $^{51}$V NMR spectroscopy ($\delta$ = −507, −531, −584 and −597 ppm); however, it is not very stable in solution. Therefore this is not expected to form;[88] the intensity of signals of **$V_{15}$** decreased and **$V_1$** and **$V_{10}$** formed at pH 3.5. In the present work, the DMEM medium is buffered at pH 7.4, providing **$V_1$** and other small oligomers stable at this pH (see Fig. 9). At longer incubation periods, the amounts of vanadium(v) oxovanadates increase, but even by 24 h, the speciation distribution of **$V_1$** + PV and oligomers is consistent with a much lower concentration of vanadium(v) in solution compared to the spectra of **$V_{14}$** at similar pH (see Fig. 8). The EPR spectra of **$V_{15}$** registered at ambient temperature also presented a single line centered $g$ = 1.9022 and with $\Delta_{p-p}$ = 19 G characteristic of the MV-POV.[57,86] Since the presence of vanadium(IV) in the EPR spectra is also decreasing, together this suggests that the intact **$V_{15}$** isomer is present but the low concentrations of any oxidized $V_{15}$-anions immidiately hydrolyze forming complexes with media components as suggested for the **$V_{14}$** system.

## Discussion

POMs are large polyanionic materials that have the potential to undergo both hydrolysis and redox chemistry. Although stable

and unreactive polyoxometalates have been reported to penetrate cellular membranes,[3] many of these compounds exert their action from the outside of the cell,[27] results consistent with those described here. Reports of formation of $\mathbf{V_{10}}$ inside yeast cells have placed this POV in acidic cytoplasmic vesicles and resulted in extrusion of $\mathbf{V_{10}}$ from yeast cells.[85,89] Studies in yeast (*S. cerevisiae*) documented that vanadate entered the cells much slower than the aqueous vanadium(IV).[85] Additional studies showed that the vanadate species responsible for the main inhibition of growth is the vanadate tetramer ($V_4$),[90] and that decavanadate entered in the form of mononuclear vanadium and then converted to $\mathbf{V_{10}}$ in the acidic lyposomers.[91] As shown with *Mycobacterium smegmatis* and with *Mycobacterium tuberculosis*, $\mathbf{V_{10}}$ is much more effective that $\mathbf{V_1}$ in inhibiting bacterial growth.[42] However, the large and charged $\mathbf{V_{10}}$ is found to hydrolyze smaller species upon exerting this effect. As a result, $\mathbf{V_{10}}$ is not likely to penetrate the charged membrane or interact directly with the membrane interface.

In order to obtain more information on these systems, we were interested in exploring responses of a G coupled-protein receptor, LHR, to $\mathbf{V_{10}}$ and structurally related POVs. To this end, a series of POVs with very different chemical and physical properties were investigated. The selected POVs represent two classes of water-soluble POMs, namely a homopolyoxometalate ($\mathbf{V_{10}}$) and two mixed-valence polyoxometalates ($\mathbf{V_{14}}$ and $\mathbf{V_{15}}$). The properties of these POVs are complementary, such that these studies will provide information on the biological responses of POMs with a wide spectrum of properties. $\mathbf{V_1}$ is the simple vanadate that is known to be a phosphatase inhibitor. $\mathbf{V_{10}}$ is a cluster formed from vanadium(V) atoms. $\mathbf{V_{14}}$ and $\mathbf{V_{15}}$ are redox active POVs, the latter stable in aqueous solutions while the former is not. They are versatile agents and in addition to hydrolyzing they have been reported to engage in processes involving reactive oxygen species (ROS) in *E. coli*,[27,54] and other biological system.[72,92–95] Considering the large number of POMs available and the wide range of properties possible,[2,20,27] we chose POMs with properties complementary to the $\mathbf{V_{10}}$ system that represent the multivalence of polyoxometalate compounds.

A motivating factor for these studies investigating the POV's effects on eukaryotic cells expressing LHR was the observation that $\mathbf{V_{10}}$ activates the protein kinase receptor FcεR.[30] This receptor is a protein kinase receptor as is the insulin receptor (IR) which was also found to be activated with vanadium complexes.[28,29] Although both the FcεRI and the IR are protein kinase receptors, signaling through different pathways than those used by LHR, a GPCR membrane protein, all three receptors use lipid rafts as signaling platforms where cholesterol, a key component of rafts, is present in high concentration. LHR receptors, like serotonin receptors,[96] another member of the GPCR receptor family, may require cholesterol for the receptor function. Previous studies with the insulin receptor demonstrated that $\mathbf{V_{10}}$ had similar effects to those of BMOV.[28–30] In response to selected POMs, CHO cells expressing low numbers of LHR (10 000 LHR per cell) exhibit changes in lipid packing that are associated with aggregation of LHR and an increase in intracellular cAMP levels. When receptor numbers are high and non-physiological (560 000 LHR per cell), V-compound effects on membrane lipid order are not reflected in either changes in LHR aggregation or intracellular levels of cAMP. Removing extracellular $\mathbf{V_{15}}$ by washing the cell does not fully affect lipid packing by these compounds, suggesting that only some V-compounds are readily available for removal; this opens the possibility that some V-compounds remain tightly associated with the cell membrane.

Before considering the effects of the three POVs and $\mathbf{V_1}$ we examined the stability and speciation of these compounds in aqueous stock solution and in media. These measurements were done using $^{51}$V NMR and EPR spectroscopy and compared to species formed in Table 2. Specifically, a summary of signals observed under the condition of the assays and in aqueous solutions at pH 7.4 are listed. The summary reflects the fact that the $\mathbf{V_{10}}$ concentration is decreasing rapidly; at the 0 h time point, 80% is present whereas less than 5% $\mathbf{V_{10}}$ is present at 24 h. Similarly, $\mathbf{V_{14}}$ is partially decomposed at $t$ = 0 and none is present at $t$ = 24 h. In contrast, $\mathbf{V_{15}}$ is present at 0 and 24 h in DMEM with a trace amount of a V(IV)-species at $t$ = 0, persisting at trace levels until 24 h. Since $VO^{2+}$ dimerizes and is not observable by EPR spectroscopy at pH 7, this signal reflects some complexation between a V(IV) compound and a media component. Considering the presence of phosphate and buffers in the assay is possible to assign this to a V(IV)-media species, indicating that the hydrolysis of the vanadium-compounds and reduction of V(V) takes place in the media at the beginning of cell treatment. Similarly, an NMR signal for $\mathbf{V_1}$ is not observed in the media but the sum of $\mathbf{V_1}$ and a phosphate–vanadate complex (PV) is observed. The $\mathbf{V_1}$ and PV signals are rapidly exchanging under these conditions. The resulting signal is abbreviated $\mathbf{V_1}$ + PV. Thus, speciation of the V-compounds in the media differs from that in aqueous solution because media components can readily form complexes with the V-compounds. Therefore, it is important to measure the spectra of the V-species formed over the time course of the cell experiments. All three POVs are present in the media at the beginning of cell treatment but, after 24 h, $\mathbf{V_{15}}$ is the only POV in significant amounts in solution although slow decomposition of $\mathbf{V_{15}}$ had started. Interestingly, no $\mathbf{V_{10}}$ formation in solution was observable indicating that any effects on cell function by $\mathbf{V_{15}}$ cannot be attributed to $\mathbf{V_{10}}$.

The three POVs and $\mathbf{V_1}$ appear to interact with the membrane lipids and decrease lipid packing, an effect that was diminished over 24 h or, for $\mathbf{V_1}$ and $\mathbf{V_{15}}$ by additional washing of cells. At any time during recovery from V-compound exposure, increased lipid disorder over baseline values appeared to affect the extent of LHR aggregation when LHR is expressed at physiologically relevant receptor numbers, *i.e.* 10 000 LHR per cell. There are no effects of lipid disorder on LHR aggregation when receptors are over-expressed in CHO cells and receptor crowding has occurred. The association of the POV with appropriately associated lipids may not require covalent binding; noncovalent interactions may be sufficient. These results are consistent with the MV-POV acting as intact entities and not through the formation of $\mathbf{V_{10}}$. For $\mathbf{V_{15}}$ this is

 

Table 2 Summary of speciation data obtained using $^{51}$V NMR and EPR spectroscopy for aqueous and cell media DMEM at $t$ = 0 and 24 h incubated with 1.0 mM of V-atoms of the listed compounds

| Anions monitored | Signals observed by $^{51}$V NMR or EPR spectroscopies | | | | | | |
|---|---|---|---|---|---|---|---|
| Compound & time/conditions | $V_1$ (%) | $V_2$ (%) | $V_4$ (%) | $V_5$ (%) | $V_{10}$ (%) | $V_{14}^V$ (%) | $V_{15}$ (%) |
| $NaVO_3$/$t$ = 0 | | | | | | | — |
| Aqueous | $V_1$ (81.9) | $V_2$ (16.4) | $V_4$ (1.64) | — | — | — | — |
| Media | PV (81.5) | $V_2$ (12.0) | $V_4$ (6.50) | — | — | — | |
| $NaVO_3$/$t$ = 24 | | | | | | | — |
| Aqueous | $V_1$ (80.0) | $V_2$ (16.0) | $V_4$ (4.00) | — | — | — | — |
| Media | PV (80.0) | $V_2$ (12.0) | $V_4$ (8.00) | — | — | — | |
| **$V_{10}$**/$t$ = 0 | | | | | | | — |
| Aqueous | $V_1$ (14.6) | $V_2$ (10.7) | $V_4$ (17.6) | $V_5$ (0.21) | $V_{10}$ (56.9) | — | — |
| Media | PV (7.54) | $V_2$ (2.11) | $V_4$ (1.05) | — | $V_{10}$ (89.3) | — | |
| **$V_{10}$**/$t$ = 24 | | | | | | | — |
| Aqueous | $V_1$ (13.7) | $V_2$ (10.5) | $V_4$ (28.4) | — | $V_{10}$ (47.3) | — | — |
| Media | PV (20.6) | $V_2$ (12.6) | $V_4$ (56.7) | $V_5$ (5.37) | $V_{10}$ (5.00) | — | |
| **$V_{14}$**/$t$ = 0 | | | | | | | — |
| Aqueous | $V_1$ (26.4) | $V_2$ (12.9) | $V_4$ (19.6) | — | $V_{10}$ (18.8) | $V_{14}^V$ (22.2) | — |
| Media | PV (44.9) | $V_2$ (11.3) | $V_4$ (14.0) | $V_5$ (3.14) | $V_{10}$ (27.0) | — | |
| **$V_{14}$**/$t$ = 24 | | | | | | | — |
| Aqueous | $V_1$ (17.4) | $V_2$ (11.8) | $V_4$ (17.3) | — | $V_{10}$ (9.20) | $V_{14}^V$ (44.3) | — |
| Media | PV (14.4) | $V_2$ (11.3) | $V_4$ (66.9) | $V_5$ (7.36) | — | — | |
| **$V_{15}$**/$t$ = 0 | | | | | | | ND |
| Aqueous | $V_1$ (31.1) | $V_2$ (24.9) | $V_4$ (44.0) | — | — | — | ND |
| Media | PV (73.0) | $V_2$ (16.0) | $V_4$ (10.9) | — | — | — | |
| **$V_{15}$**/$t$ = 24 | | | | | | — | ND |
| Aqueous | $V_1$ (30.5) | $V_2$ (23.8) | $V_4$ (45.6) | — | — | — | ND |
| Media | PV (44.6) | $V_2$ (16.9) | $V_4$ (36.0) | $V_5$ (2.67) | — | — | |

Compounds examined are $NaVO_3$ as **$V_1$**; $[Na_2(H_2O)_{10}][H_3V_{10}O_{28}\{Na(H_2O)_2\}]\cdot 3H_2O$ as **$V_{10}$**; $K(NH_4)_4[H_6V_{14}O_{38}(PO_4)]\cdot 11H_2O$ as **$V_{14}$** and $[(CH_3)_4N]_6[V_{15}O_{36}(Cl)]$ as **$V_{15}$**; any form of reduced vanadium is listed as V(IV), so for **$V_{15}$** the V(IV) correspond to the sum of the V(IV) in the MV-POV and in mononuclear V(IV) soluble in the media; — not present; PV stands for vanadium–phosphate complex in rapid equilibrium with **$V_1$** ($H_2VO_4^-$); trace – barely detectable; ND – not detectable by the techniques. Aqueous solution $^{51}$V NMR and EPR spectra are presented in the ESI. The % were calculated using the $^{51}$V NMR spectra signal integrals and are an approximation, considering the systems contain V(V) and V(IV) species.

particularly clear because part of **$V_{15}$** is intact at the end of the incubation. The migration of LHR from the bulk membrane, the site of POV or **$V_1$** interactions with membrane lipids, to the membrane microdomains with more densely packed lipids effectively concentrates receptors. This concentration of receptors in membrane microdomains, as demonstrated for BMOV or $VOSO_4$, produces LHR aggregation and activation of receptors, which then signal intracellularly.[41] Although it appears that the POVs and **$V_1$** are cleared from the membrane in approximately 24 h, it is not clear what happens to the V-compounds over this time. We have monitored the POVs and **$V_1$** in the media using both EPR and $^{51}$V NMR spectroscopies but cannot monitor events in the cell membrane.

Because speciation of these compounds is complex and time-dependent, the interactions between these various vanadium compounds and CHO cell membranes are likely to vary with time. This makes modeling of vanadium compounds more complex and dependent on the vanadium species available. Fig. 10 shows various proposed mechanisms involved in vanadium compound interactions with cells that could potentially lead to the effects of these compounds on LHR signaling. At any time, because multiple species form, it is unlikely that only one type of interaction is occurring. Rather, some species may interact with cells as shown in (a), while others are interacting through mechanisms summarized in (b) and (c). Fig. 10a demonstrates the interactions occurring for compounds, like **$V_{14}$** and **$V_{15}$**, that can interact with extracellular structures but, due to their hydrophobicity, are less likely to insert in lipid bilayers. It is not known from these experiments whether these compounds can sufficiently perturb membrane structures or drive the concentration of LHR in membrane microdomains that provide locally favorable conditions for LHR signal transduction. However, speciation of these compounds may be sufficient to produce vanadium-containing compounds that are more lipophilic (b) and thus more likely to interact with the lipid bilayer. Such lipophilic compounds may, at least in part, be responsible for the changes in lipid packing that are observed in cells and for LHR concentration in membrane rafts. Lipid bilayer interactions of lipophilic species and internalization of these V-compounds is attractive from a functional perspective given that phosphatase targets for these compounds are found in the cell cytoplasm.[48] More importantly, membrane transport *via* an unidentified mechanism may be available for transport of these compounds into the CHO cell interior. For many compounds functioning as drugs, the ability to transit the plasma membrane, enter the cell cytoplasm and then target intracellular functions or structures, is critical to their action.[97] Transport of V-compounds across a membrane would likely depend on available membrane transporters that could be adapted for the transport of these V-compounds.[96] In the case of the erythrocyte membrane, the addition of DIDS stopped the internalization of some organic V-compounds.[98,99] Alternatively, lipoidal diffusion is commonly considered as an alternative explanation for drug movement across membrane barriers (reviewed in ref. 100 and 101). Drugs proposed to use lipoidal transport display, in monolayers, approximately equal rates

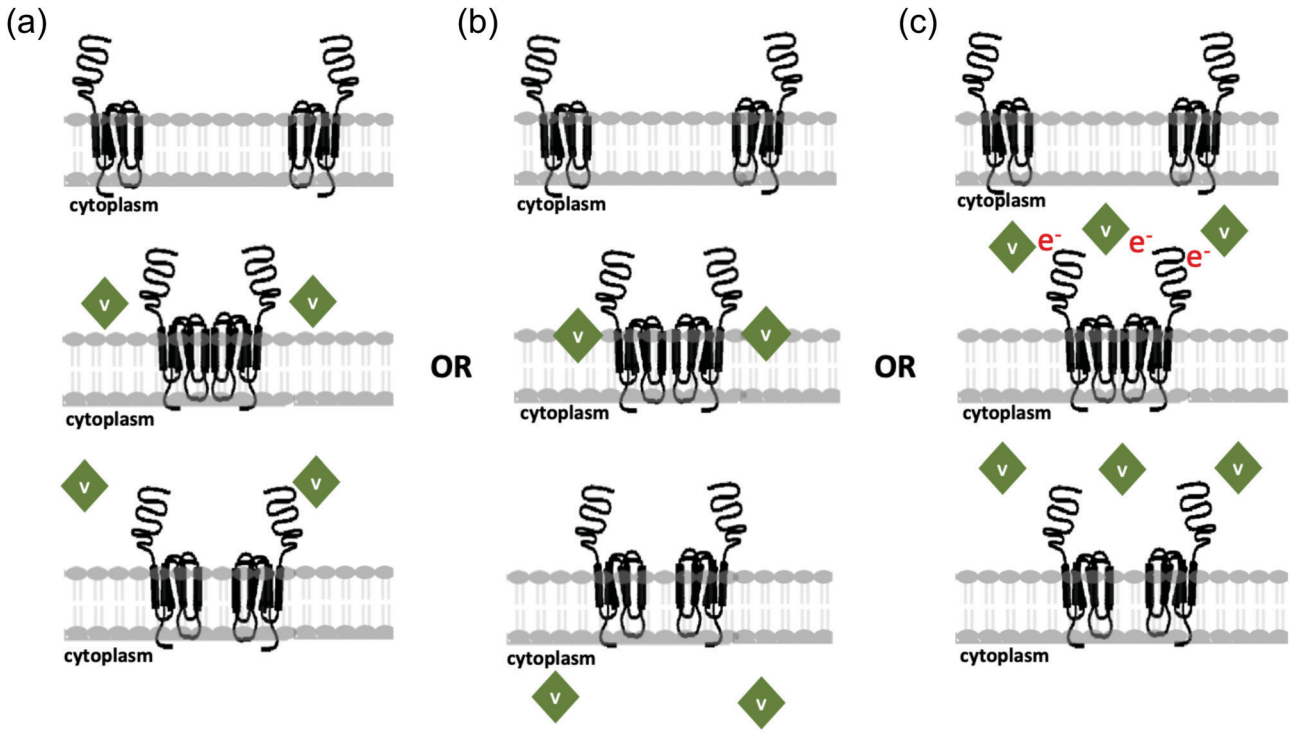


Fig. 10 Models for the alternative modes of action of the vanadium compounds on cell membranes where cells express 10 000 LHR per cell, a comparatively low receptor density. (a) V-Compounds interact with CHO cell membranes and are not internalized; (b) V-compounds impact the lipid bilayer followed by POV hydrolysis and internalization of the resulting species; or (c) POVs exert the effects through an electron transfer process.

of flux across the monolayer in either direction. These compounds have "intrinsic permeability" in cell lines expressing membrane transporters used for passive diffusion.

It is also possible that select vanadium species interact with extracellular components impacting the lipid bilayer and, more important, these interactions are followed by POV hydrolysis and internalization of the resulting POV species (see Fig. 10b). POV compounds such as $\mathbf{V_{10}}$ have been explored in animal studies as glucose-regulating drugs for oral use.[14,102,103] In accordance with Lipinski's rules[104,105] describing requirements for an ideal drug capable of crossing membranes, small and neutral compounds, such as BMOV, can penetrate membranes[29] unlike the POVs described here. In addition to interacting with membrane surfaces, if sufficiently hydrophilic, vanadium compounds, such as BMOV, may also dissolve in the hydrophobic core of the bilayer. $VOSO_4$, on the other hand, readily penetrates interfaces over the course of a few minutes and is internalized using available cation transporters.[85] If the POVs or $\mathbf{V_1}$ are transiently associated with membrane lipids and then internalized, as was reported for BMOV or $VOSO_4$, the resulting removal from the cells by washing would appear to be slow. Considering the known locations of the POVs being outside the cells, it was surprising that $\mathbf{V_{15}}$ was not readily removed by additional cell washes. Importantly, $\mathbf{V_1}$ was also not readily removed, presumably reflecting the possibility that it is internalized. It is, however, possible that the $\mathbf{V_{15}}$ and the two other POVs internalize after hydrolysis.

Finally, the propensity of $\mathbf{V_{14}}$ and $\mathbf{V_{15}}$ to engage in processes related to formation of ROS due to their large size and charges, as well as the possibility that they act without membrane penetration, allow us to test whether compounds with properties that differ from simple vanadium coordination complexes are able to induce signal transduction by LHR, presumably as a result inactive to active conformational changes. Interestingly, some V(IV), albeit at trace levels, formed initially at the beginning of growth in all samples including samples treated with $\mathbf{V_1}$, $\mathbf{V_{10}}$ and V(IV)-containing $\mathbf{V_{14}}$ and $\mathbf{V_{15}}$. V(V) conversion to V(IV) is accompanied by abstraction of electrons and, in the process, generates ROS. This has been documented in multiple systems treated with vanadium(V) compounds as well as vanadium(IV) compounds that generate an electron upon oxidation to vanadium(V). It is interesting to consider that conformational changes and G-protein activation in LHR leading to signal transduction may involve ROSs. The POVs are significantly different than all the other vanadium compounds that have been reported to affect lipid organization or activation of the LHR or insulin receptors because the potential for direct interactions of POVs with LHR is reduced. In these studies, we considered whether a ROS-mechanism might impact some of the necessary steps in place of, or in addition to, a potential mechanism as a phosphatase inhibitor or a direct interaction between the lipids and the compounds causing changes in LHR conformation, promotion of LHR aggregation, and subsequent signaling. Demonstration that a large vanadium compound that is less likely to act as a phosphatase inhibitor gave credence to alternative mechanisms. However, as noted above, none of these mechanisms are happening exclusively simply

 

because of the complex nature of vanadium compound speciation and the multitude of cellular environments with proteins, nucleic acids, lipids and other metabolites.

## Conclusions

These studies demonstrate that the interactions of three POVs and $\mathbf{V_1}$ with the eukaryotic cell plasma membrane directly decrease the packing of membrane lipids and, as an indirect effect, drive aggregation of LHR, a G protein-coupled receptor in CHO cells. LHR continues to be aggregated when lipid order is decreased in the presence of $\mathbf{V_{10}}$ and $\mathbf{V_{15}}$ in the cell medium and even after the $\mathbf{V_1}$ or $\mathbf{V_{15}}$ have been removed. Importantly, these effects are only observed on cells where LHR protein density is low; when LHR is overexpressed, receptor density is high and the receptors are constitutively aggregated regardless of $\mathbf{V_{10}}$, $\mathbf{V_{14}}$ and $\mathbf{V_{15}}$ effects on membrane lipid packing. In the case of other small V-compounds that are known to traverse membranes, we anticipate that they are taken up by cells and appear in the cell cytoplasm. However, this process is considerably more complex for $\mathbf{V_{10}}$, $\mathbf{V_{14}}$, and $\mathbf{V_{15}}$ that are large molecules with high charges and not likely to readily traverse membranes. Indeed, studies with model membranes and $\mathbf{V_{10}}$ show that it resides away from the interface in the aqueous layer. Although these POVs may hydrolyze and internalize as smaller vanadate-containing molecules in such cases, one would not anticipate that the most stable POV derivative would be the most effective compound. The speciation studies showed the presence of vanadium(IV) compounds and thus documented the potential for at least partial involvement of ROS and electron transfer processes in cells. These studies document the ability of a wide range of vanadium compounds to initiate signal transduction including compounds that do not readily transverse membranes and further investigation of these effects are warranted.

## Conflicts of interest

There are no conflicts to declare.

## Acknowledgements

DA would like to thank King Faisal University and the Saudi Arabian Cultural Mission for her fellowship to study at Colorado State University. KP and GGN thank the Coordenação de Aperfeiçoamento de Pessoal de Nível Superior (CAPES) and CAPES/PrInt program for the scholarship supporting KP's visit to Colorado State University. DCC and DR thank Colorado State University for support. DCC also thank the Arthur Cope Scholar Foundations administered by the American Chemical Society for partial support. We also thank Dr Chris Rithner for assistance in obtaining spectroscopic measurements in the Central Instrument Facility. We thank Professor Sandra Eaton for helpful discussions on recording and interpretation of EPR spectra.

## References

1 N. Chahin, L. A. Uribe, A. M. Debela, S. Thorimbert, B. Hasenknopf, M. Ortiz, I. Katakis and C. K. O'Sullivan, Electrochemical primer extension based on polyoxometalate electroactive labels for multiplexed detection of single nucleotide polymorphisms, *Biosens. Bioelectron.*, 2018, **117**, 201–206.
2 M. T. Pope and A. Müller, Polyoxometalate chemistry: an old field with new dimensions in several disciplines, *Angew. Chem., Int. Ed. Engl.*, 1991, **30**, 34–48.
3 J. T. Rhule, C. L. Hill, D. A. Judd and R. F. Schinazi, Polyoxometalates in medicine, *Chem. Rev.*, 1998, **98**, 327–358.
4 M. Stuckart and K. Y. Monakhov, Polyoxometalates as components of supramolecular assemblies, *Chem. Sci.*, 2019, **10**, 4364–4376.
5 A. Bergeron, K. Kostenkova, M. Selman, H. A. Murakami, E. Owens, N. Haribabu, R. Arulanandam, J.-S. Diallo and D. C. Crans, Enhancement of oncolytic virotherapy by vanadium(V) dipicolinates, *Biometals*, 2019, **32**, 545–561.
6 B. E. Petel and E. M. Matson, Conversion of NO x 1−(x= 2, 3) to NO using an oxygen-deficient polyoxovanadate–alkoxide cluster, *Chem. Commun.*, 2020, **56**, 555–558.
7 H. Stephan, M. Kubeil, F. Emmerling and C. E. Müller, Polyoxometalates as versatile enzyme inhibitors, *Eur. J. Inorg. Chem.*, 2013, 1585–1594.
8 S. Ramos, M. Manuel, T. Tiago, R. Duarte, J. Martins, C. Gutiérrez-Merino, J. J. Moura and M. Aureliano, Decavanadate interactions with actin: inhibition of G-actin polymerization and stabilization of decameric vanadate, *J. Inorg. Biochem.*, 2006, **100**, 1734–1743.
9 N. Samart, J. Saeger, K. J. Haller, M. Aureliano and D. C. Crans, Interaction of decavanadate with interfaces and biological model membrane systems: Characterization of soft oxometalate systems, *J. Mol. Eng. Mater.*, 2014, **2**, 1440007.
10 J. Breibeck, N. I. Gumerova, B. B. Boesen, M. Galanski and A. Rompel, Keggin-type polyoxotungstates as mushroom tyrosinase inhibitors-A speciation study, *Sci. Rep.*, 2019, **9**, 5183.
11 A. Sap, L. Vandebroek, V. Goovaerts, E. Martens, P. Proost and T. N. Parac-Vogt, Highly selective and tunable protein hydrolysis by a polyoxometalate complex in surfactant solutions: a step toward the development of artificial metalloproteases for membrane proteins, *ACS Omega*, 2017, **2**, 2026–2033.
12 T. J. Paul, T. N. Parac-Vogt, D. Quiñonero and R. Prabhakar, Investigating Polyoxometalate–Protein Interactions at Chemically Distinct Binding Sites, *J. Phys. Chem. B*, 2018, **122**, 7219–7232.
13 R. Raza, A. Matin, S. Sarwar, M. Barsukova-Stuckart, M. Ibrahim, U. Kortz and J. Iqbal, Polyoxometalates as potent and selective inhibitors of alkaline phosphatases with profound anticancer and amoebicidal activities, *Dalton Trans.*, 2012, **41**, 14329–14336.
14 M. Aureliano and D. C. Crans, Decavanadate ($V_{10}O_{28}^{6-}$) and oxovanadates: Oxometalates with many biological activities, *J. Inorg. Biochem.*, 2009, **103**, 536–546.

15 A. Tocilj, F. Schlünzen, D. Janell, M. Glühmann, H. A. Hansen, J. Harms, A. Bashan, H. Bartels, I. Agmon, F. Franceschi and A. Yonath, The small ribosomal subunit from Thermus thermophilus at 4.5 Å resolution: pattern fittings and the identification of a functional site, *Proc. Natl. Acad. Sci. U. S. A.*, 1999, **96**, 14252–14257.

16 F. Schluenzen, A. Tocilj, R. Zarivach, J. Harms, M. Gluehmann, D. Janell, A. Bashan, H. Bartels, I. Agmon, F. Franceschi and A. Yonath, Structure of functionally activated small ribosomal subunit at 3.3 Å resolution, *Cell*, 2000, **102**, 615–623.

17 A. Bijelic and A. Rompel, The use of polyoxometalates in protein crystallography–An attempt to widen a well-known bottleneck, *Coord. Chem. Rev.*, 2015, **299**, 22–38.

18 D. C. Crans, I. Sánchez-Lombardo and C. C. McLauchlan, Exploring Wells-Dawson Clusters Associated With the Small Ribosomal Subunit, *Front. Chem.*, 2019, **7**, 462.

19 T. Yamase, Anti-tumor, -viral, and -bacterial activities of polyoxometalates for realizing an inorganic drug, *J. Mater. Chem.*, 2005, **15**, 4773–4782.

20 B. Hasenknopf, Polyoxometalates: introduction to a class of inorganic compounds and their biomedical applications, *Front. Biosci.*, 2005, **10**, 10.2741.

21 D. Marques-da-Silva, G. Fraqueza, R. Lagoa, A. A. Vannathan, S. S. Mal and M. Aureliano, Polyoxovanadate inhibition of Escherichia coli growth shows a reverse correlation with Ca 2 + -ATPase inhibition, *New J. Chem.*, 2019, **43**, 17577–17587.

22 H. G. T. Ly, T. T. Mihaylov, P. Proost, K. Pierloot, J. N. Harvey and T. N. Parac-Vogt, Chemical Mimics of Aspartate-Directed Proteases: Predictive and Strictly Specific Hydrolysis of a Globular Protein at $Asp^{-}$ X Sequence Promoted by Polyoxometalate Complexes Rationalized by a Combined Experimental and Theoretical Approach, *Chem. – Eur. J.*, 2019, **25**, 14370–14381.

23 A. Bijelic, M. Aureliano and A. Rompel, Polyoxometalates as potential next-generation metallodrugs in the combat against cancer, *Angew. Chem., Int. Ed.*, 2019, **58**, 2980–2999.

24 M. Ortiz, A. M. Debela, M. Svobodova, S. Thorimbert, D. Lesage, R. B. Cole, B. Hasenknopf and C. K. O'Sullivan, PCR Incorporation of Polyoxometalate Modified Deoxynucleotide Triphosphates and Their Application in Molecular Electrochemical Sensing of Yersinia pestis, *Chem. – Eur. J.*, 2017, **23**, 10597–10603.

25 J. H. Bae, E. D. Lew, S. Yuzawa, F. Tome, I. Lax and J. Schlessinger, The selectivity of receptor tyrosine kinase signaling is controlled by a secondary SH2 domain binding site, *Cell*, 2009, **138**, 514–524.

26 R. L. Felts, T. J. Reilly and J. J. Tanner, Structure of Francisella tularensis AcpA prototype of a unique superfamily of acid phosphatases and phospholipases C, *J. Biol. Chem.*, 2006, **281**, 30289–30298.

27 A. Bijelic, M. Aureliano and A. Rompel, The antibacterial activity of polyoxometalates: structures, antibiotic effects and future perspectives, *Chem. Commun.*, 2018, **54**, 1153–1169.

28 A. Al-Qatati, P. Winter, A. Wolf-Ringwall, P. Chatterjee, A. Van Orden, D. C. Crans, D. A. Roess and B. G. Barisas, Insulin Receptors and Downstream Substrates Associate with Membrane Microdomains after Treatment with Insulin or Chromium(III) Picolinate, *Cell Biochem. Biophys.*, 2012, 1–10.

29 P. W. Winter, A. Al-Qatati, A. L. Wolf-Ringwall, S. Schoeberl, P. B. Chatterjee, B. G. Barisas, D. A. Roess and D. C. Crans, The anti-diabetic bis (maltolato) oxovanadium (IV) decreases lipid order while increasing insulin receptor localization in membrane microdomains, *Dalton Trans.*, 2012, **41**, 6419–6430.

30 A. Al-Qatati, F. L. Fontes, B. G. Barisas, D. Zhang, D. A. Roess and D. C. Crans, Raft localization of Type I Fcε receptor and degranulation of RBL-2H3 cells exposed to decavanadate, a structural model for $V_2O_5$, *Dalton Trans.*, 2013, **42**, 11912–11920.

31 N. Samart, D. Althumairy, D. Zhang, D. A. Roess and D. C. Crans, Initiation of a novel mode of membrane signaling: Vanadium facilitated signal transduction, *Coord. Chem. Rev.*, 2020, **416**, 213–286.

32 M. Ascoli, F. Fanelli and D. Segaloff, The lutropin/choriogonadotropin receptor, a 2002 perspective, *Endocr. Rev.*, 2002, **23**, 141–174.

33 G.-M. Hu, T.-L. Mai and C.-M. Chen, Visualizing the GPCR network: Classification and evolution, *Sci. Rep.*, 2017, **7**, 15495.

34 M. Ascoli, *Luteinizing Hormone Action and Receptors*, CRC Press, 2019.

35 Y. Kang, O. Kuybeda, P. W. de Waal, S. Mukherjee, N. Van Eps, P. Dutka, X. E. Zhou, A. Bartesaghi, S. Erramilli and T. Morizumi, Cryo-EM structure of human rhodopsin bound to an inhibitory G protein, *Nature*, 2018, **558**, 553.

36 V. Cherezov, D. M. Rosenbaum, M. A. Hanson, S. G. Rasmussen, F. S. Thian, T. S. Kobilka, H.-J. Choi, P. Kuhn, W. I. Weis and B. K. Kobilka, High-resolution crystal structure of an engineered human β2-adrenergic G protein–coupled receptor, *Science*, 2007, **318**, 1258–1265.

37 A. Ulloa-Aguirre, T. Zariñán, E. Jardón-Valadez, R. Gutiérrez-Sagal and J. A. Dias, Structure-Function Relationships of the Follicle-Stimulating Hormone Receptor, *Front. Endocrinol.*, 2018, **9**, 707.

38 S. M. Smith, Y. Lei, J. Liu, M. E. Cahill, G. M. Hagen, B. G. Barisas and D. A. Roess, Luteinizing hormone receptors translocate to plasma membrane microdomains after binding of human chorionic gonadotropin, *Endocrinology*, 2006, **147**, 1789–1795.

39 Y. Lei, G. M. Hagen, S. M. L. Smith, J. Liu, B. G. Barisas and D. A. Roess, Constitutively-active human LH receptors are self-associated and localized in rafts, *Mol. Cell. Endocrinol.*, 2007, **260-262**, 65–72.

40 A. L. Wolf-Ringwall, P. W. Winter, D. A. Roess and B. G. Barisas, Luteinizing Hormone Receptors are Confined in Mesoscale Plasma Membrane Microdomains Throughout Recovery from Receptor Desensitization, *Cell Biochem. Biophys.*, 2014, **68**, 561–569.

41 D. Althumairy, H. A. Murakami, D. Zhang, B. G. Barisas, D. A. Roess and D. C. Crans, Effects of vanadium (IV)

 

compounds on plasma membrane lipids leads to G protein-coupled receptor signal transduction, *J. Inorg. Biochem.*, 2019, 110873.

42 N. Samart, Z. Arhouma, S. Kumar, H. A. Murakami, D. C. Crick and D. C. Crans, Decavanadate inhibits microbacterial growth more potently than other oxovanadates, *Front. Chem.*, 2018, **6**, 519.

43 D. C. Crans, K. A. Woll, K. Prusinskas, M. D. Johnson and E. Norkus, Metal speciation in health and medicine represented by iron and vanadium, *Inorg. Chem.*, 2013, **52**, 12262–12275.

44 A. Levina, D. C. Crans and P. A. Lay, Speciation of metal drugs, supplements and toxins in media and bodily fluids controls in vitro activities, *Coord. Chem. Rev.*, 2017, **352**, 473–498.

45 J. Stover, C. D. Rithner, R. A. Inafuku, D. C. Crans and N. E. Levinger, Interaction of dipicolinatodioxovanadium(V) with polyatomic cations and surfaces in reverse micelles, *Langmuir*, 2005, **21**, 6250–6258.

46 D. C. Crans, Antidiabetic, Chemical, and Physical Properties of Organic Vanadates as Presumed Transition-State Inhibitors for Phosphatases, *J. Org. Chem.*, 2015, **80**, 11899–11915.

47 D. C. Crans, C. D. Rithner, B. Baruah, B. L. Gourley and N. E. Levinger, Molecular probe location in reverse micelles determined by NMR dipolar interactions, *J. Am. Chem. Soc.*, 2006, **128**, 4437–4445.

48 A. Chatkon, P. B. Chatterjee, M. A. Sedgwick, K. J. Haller and D. C. Crans, Counterion affects interaction with interfaces: The antidiabetic drugs metformin and decavanadate, *Eur. J. Inorg. Chem.*, 2013, 1859–1868.

49 D. C. Crans, S. Schoeberl, E. Gaidamauskas, B. Baruah and D. A. Roess, Antidiabetic vanadium compound and membrane interfaces: interface-facilitated metal complex hydrolysis, *J. Biol. Inorg. Chem.*, 2011, **16**, 961–972.

50 D. C. Crans, B. Baruah, A. Ross and N. E. Levinger, Impact of confinement and interfaces on coordination chemistry: Using oxovanadate reactions and proton transfer reactions as probes in reverse micelles, *Coord. Chem. Rev.*, 2009, **253**, 2178–2185.

51 I. Sanchez-Lombardo, B. Baruah, S. Alvarez, K. R. Werst, N. A. Segaline, N. E. Levinger and D. C. Crans, Size and Shape Trump Charge in Interactions of Oxovanadates with Self-assembled Interfaces: Application of Continuous Shape Measure Analysis to the Decavanadate Anion, *New J. Chem.*, 2016, **40**, 962–975.

52 B. Baruah, J. M. Roden, M. A. Sedgwick, N. M. Correa, D. C. Crans and N. E. Levinger, When is Water Not Water? Exploring Water Confined in Large Reverse Micelles Using a Highly Charged Inorganic Molecular Probe, *J. Am. Chem. Soc.*, 2006, **128**, 12758–12765.

53 K. Postal, D. Maluf, G. Valdameri, A. Rüdiger, D. Hughes, E. de Sá, R. Ribeiro, E. de Souza, J. Soares and G. Nunes, Chemoprotective activity of mixed valence polyoxovanadates against diethylsulphate in E. coli cultures: insights from solution speciation studies, *RSC Adv.*, 2016, **6**, 114955.

54 H. K. Daima, P. Selvakannan, R. Shukla, S. K. Bhargava and V. Bansal, Fine-tuning the antimicrobial profile of biocompatible gold nanoparticles by sequential surface functionalization using polyoxometalates and lysine, *PLoS One*, 2013, **8**, e79676.

55 T. Duraisamy, A. Ramanan and J. Vittal, Novel self-assembled decavanadate clusters forming 1D molecular chains and 2D molecular arrays:[HMTA-H···H2O][HMTA-CH2OH][H3V10O28 {Na (H2O) 4}]·4H2O and [Na2 (H2O) 10][H3V10O28 {Na (H2O) 2}]·3H2O, *Cryst. Eng.*, 2000, **3**, 237–250.

56 S. Yerra, B. K. Tripuramallu and S. K. Das, Decavanadate-based discrete compound and coordination polymer: Synthesis, crystal structures, spectroscopy and nanomaterials, *Polyhedron*, 2014, **81**, 147–153.

57 G. G. Nunes, A. C. Bonatto, G. Carla, A. Barison, R. R. Ribeiro, D. F. Back, A. V. C. Andrade, E. L. de Sá, O. Pedrosa Fde and J. F. Soares, Synthesis, characterization and chemoprotective activity of polyoxovanadates against DNA alkylation, *J. Inorg. Biochem.*, 2012, **108**, 36–46.

58 L. Jin, A. Millard, J. Wuskell, H. Clark and K. Loew, Cholesterol-enriched lipid domains can be visualized by di-4-ANEPPDHQ with linear and nonlinear optics, *Biophys. J.*, 2005, **90**, 2563–2575.

59 D. M. Owen, P. M. P. Lanigan, C. Dunsby, I. Munro, D. Grant, M. A. A. Neil, P. M. W. French and A. Magee, Fluorescence lifetime imaging provides enhanced contrast when imaging the phase-sensitive dye di-4-ANEPPDHQ in model membranes and live cells, *Biophys. J.*, 2006, **90**, L80–L82.

60 J. Dinic, H. Biverståhl, L. Mäler and I. Parmryd, Laurdan and di-4-ANEPPDHQ do not respond to membrane-inserted peptides and are good probes for lipid packing, *Biochim. Biophys. Acta, Biomembr.*, 2011, **1808**, 298–306.

61 D. M. Owen, C. Rentero, A. Magenau, A. Abu-Siniyeh and K. Gaus, Quantitative imaging of membrane lipid order in cells and organisms, *Nat. Protoc.*, 2012, **7**, 24–35.

62 D. W. Piston and M. A. Rizzo, in *Fluorescent Proteins*, ed. K. F. Sullivan, 2nd edn, 2008, vol. 85, pp. 415–430.

63 Á. Szabó, G. Horváth, J. Szöllősi and P. Nagy, Quantitative characterization of the large-scale association of ErbB1 and ErbB2 by flow cytometric homo-FRET measurements, *Biophys. J.*, 2008, **95**, 2086–2096.

64 M. Tramier, T. Piolot, I. Gautier, V. Mignotte, J. Coppey, K. Kemnitz, C. Durieux and M. Coppey-Moisan, *Methods in Enzymology*, Elsevier, 2003, vol. 360, pp. 580–597.

65 M. Tramier and M. Coppey-Moisan, Fluorescence anisotropy imaging microscopy for homo-FRET in living cells, *Methods Cell Biol.*, 2008, **85**, 395–414.

66 E. K. L. Yeow and A. H. A. Clayton, Enumeration of Oligomerization States of Membrane Proteins in Living Cells by Homo-FRET Spectroscopy and Microscopy: Theory and Application, *Biophys. J.*, 2007, **92**, 3098–3104.

67 L. M. DiPilato and J. Zhang, The role of membrane microdomains in shaping [small beta]2-adrenergic receptor-mediated cAMP dynamics, *Mol. BioSyst.*, 2009, **5**, 832–837.

68 D. C. Crans, C. D. Rithner and L. A. Theisen, Application of time-resolved vanadium-51 2D NMR for quantitation of

kinetic exchange pathways between vanadate monomer, dimer, tetramer, and pentamer, *J. Am. Chem. Soc.*, 1990, **112**, 2901–2908.

69 M. T. Pope and B. W. Dale, Isopoly -vanadates, -niobates and –tantalates, *Q. Rev., Chem. Soc.*, 1968, **22**, 527–548.

70 N. D. Chasteen, in *Structure and Bonding*, ed. M. J. Clarke, J. B. Goodenough, J. A. Ibers, C. K. Jørgensen, D. M. P. Mingos, J. B. Neilands, G. A. Palmer, D. Reinen, P. J. Sadler, R. Weiss and R. J. P. Williams, Springer-Verlag, New York, 1983, Biochemistry of Vanadium, vol. 53, pp. 105–138.

71 A. Levina, A. I. McLeod, S. J. Gasparini, A. Nguyen, W. G. M. De Silva, J. B. Aitken, H. H. Harris, C. Glover, B. Johannessen and P. A. Lay, Reactivity and Speciation of Anti-Diabetic Vanadium Complexes in Whole Blood and Its Components: The Important Role of Red Blood Cells, *Inorg. Chem.*, 2015, **54**, 7753–7766.

72 D. C. Crans, N. E. Barkley, L. Montezinho and M. M. Castro, *Metal-based Anticancer Agents*, 2019, pp. 169–195.

73 K. A. Doucette, K. N. Hassell and D. C. Crans, Selective speciation improves efficacy and lowers toxicity of platinum anticancer and vanadium antidiabetic drugs, *J. Inorg. Biochem.*, 2016, **165**, 56–70.

74 C. F. Baes and R. S. Mesmer, *The Hydrolysis of Cations*, John Wiley & Sons, New York, 1976.

75 L. Pettersson, B. Hedman, I. Andersson and N. Ingri, Multicomponent polyanions. 34. A potentiomtric and V-51 NMR-study of equilibria in the $H^{+}$-$HVO_4^{2-}$ system in 0.6 M Na(Cl) medium covering the range 1 less-than-or-equal-to-1G [H +] less to 10, *Chem. Scr.*, 1983, **22**, 254–264.

76 L. Pettersson, I. Andersson and B. Hedman, Multicomponent polyanions. 37. A potentiomtric and V-51 NMR-study of equilibria in the $H^{+}$-$HVO_4^{2-}$ system in 0.6 M Na($ClO_4$) medium covering the range 1 less-than-or-equal-to-1G [H +] less-than-or-equal-to 10, *Chem. Scr.*, 1985, **25**, 309–317.

77 M. J. Gresser, A. S. Tracey and K. M. Parkinson, Vanadium (V) oxyanions: the interaction of vanadate with pyrophosphate, phosphate, and arsenate, *J. Am. Chem. Soc.*, 1986, **108**, 6229–6234.

78 T. Kiss, T. Jakusch, D. Hollender, A. Dornyei, E. A. Enyedy, J. C. Pessoa, H. Sakurai and A. Sanz-Medel, Biospeciation of antidiabetic VO(IV) complexes, *Coord. Chem. Rev.*, 2008, **252**, 1153–1162.

79 D. Sanna, J. Palomba, G. Lubinu, P. Buglyó, S. Nagy, F. Perdih and E. Garribba, Role of ligands in the uptake and reduction and reduction of V(V) complexes in red blood cells, *Med. Chem.*, 2019, **62**, 654–664.

80 D. C. Crans, J. J. Smee, E. Gaidamauskas and L. Yang, The chemistry and biochemistry of vanadium and the biological activities exerted by vanadium compounds, *Chem. Rev.*, 2004, **104**, 849–902.

81 J. C. Pessoa, Thirty years through vanadium chemistry, *J. Inorg. Biochem.*, 2015, **147**, 4–24.

82 S. S. Amin, K. Cryer, B. Zhang, S. K. Dutta, S. S. Eaton, O. P. Anderson, S. M. Miller, B. A. Reul, S. M. Brichard and D. C. Crans, Chemistry and insulin-mimetic properties of bis(acetylacetonate)oxovanadium(IV) and derivatives, *Inorg. Chem.*, 2000, **39**, 406–416.

83 R. D. Horvat, S. Nelson, C. M. Clay, B. G. Barisas and D. A. Roess, Intrinsically fluorescent luteinizing hormone receptor demonstrates hormone-driven aggregation, *Biochem. Biophys. Res. Commun.*, 1999, **255**, 382–385.

84 D. Althumairy, D. A. Roess and B. G. Barisas, Effects of Luteinizing Hormone Receptor Expression Level on Receptor Aggregation and Function, *Biophys. J.*, 2020, **118**, 95a.

85 G. R. Willsky, D. A. White and B. C. McCabe, Metabolism of added orthovanadate to vanadyl and high-molecular-weight vanadates by Saccharomyces cerevisiae, *J. Biol. Chem.*, 1984, **259**, 13273–13281.

86 Y.-G. Li, Y. Lu, G.-Y. Luan, E.-B. Wang, Y.-B. Duan, C.-W. Hu, N.-H. Hu and H.-Q. Jia, Hydrothermal syntheses and crystal structures of new cage-like mixed-valent polyoxovanadates, *Polyhedron*, 2002, **21**, 2601–2608.

87 S. S. Amin, K. Cryer, B. Zhang, S. K. Dutta, S. S. Eaton, O. P. Anderson, S. M. Miller, B. A. Reul, S. M. Brichard and D. C. Crans, Chemistry and insulin-mimetic properties of bis (acetylacetonate) oxovanadium (IV) and derivatives1, *Inorg. Chem.*, 2000, **39**, 406–416.

88 D. Hou, K. S. Hagen and C. L. Hill, Pentadecavanadate, V 15 O 42 9–, a new highly condensed fully oxidized isopolyvanadate with kinetic stability in water, *J. Chem. Soc., Chem. Commun.*, 1993, 426–428.

89 G. Willsky, J. Leung, P. Offermann, E. Plotnick and S. Dosch, Isolation and characterization of vanadate-resistant mutants of Saccharomyces cerevisiae, *J. Bacteriol.*, 1985, **164**, 611–617.

90 D. C. Crans and G. Willsky, Oxovanadate and oxomolybdate cluster interactions with enzymes and whole cells The Proceedings from the 25th Steenbock Symposium, June 10–14th, University of Wisconsin-Madison, 1997, pp. 116-125.

91 D. C. Crans, B. Baruah and C. R. Murphy, Vanadium Biochemistry, ed. Manuel Aureliano Alves ''Research Signpost'', Interaction of decavanadate with model lipid interfaces, 2007, pp. 1-13.

92 U. Zor, E. Ferber, P. Gergely, K. Szücs, V. Dombradi and R. Goldman, Reactive oxygen species mediate phorbol ester-regulated tyrosine phosphorylation and phospholipase A2 activation: potentiation by vanadate, *Biochem. J.*, 1993, **295**, 879–888.

93 E. Kioseoglou, S. Petanidis, C. Gabriel and A. Salifoglou, The chemistry and biology of vanadium compounds in cancer therapeutics, *Coord. Chem. Rev.*, 2015, **301**, 87–105.

94 M. Valko, C. Rhodes, J. Moncol, M. M. Izakovic and M. Mazur, Free radicals, metals and antioxidants in oxidative stress-induced cancer, *Chem.-Biol. Interact.*, 2006, **160**, 1–40.

95 D. C. Crans, A. Trujillo, P. Pharazyn and M. Cohen, How environment affects drug activity: Localization, compartmentalization and reactions of a vanadium insulin-enhancing compound, dipicolinatooxovanadium(V), *Coord. Chem. Rev.*, 2011, **255**, 2178–2192.

96 M. Jafurulla, S. Tiwari and A. Chattopadhyay, Identification of cholesterol recognition amino acid consensus

 

(CRAC) motif in G-protein coupled receptors, *Biochem. Biophys. Res. Commun.*, 2011, **404**, 569–573.
97 T. Peck, S. Hill and M. Williams, *Drug passage across the cell membrane, Pharmacology for Anaesthesia and Intensive Care*, Greenwich Medical Media, London, 2nd edn, 2003, pp. 3–10.
98 X. Yang, K. Wang, J. Lu and D. C. Crans, Membrane transport of vanadium compounds and the interaction with the erythrocyte membrane, *Coord. Chem. Rev.*, 2003, **237**, 103–111.
99 X.-G. Yang, X.-D. Yang, L. Yuan, K. Wang and D. C. Crans, The Permeability and Cytotocxicity of Insulin-Mimetic Vanadium Compounds, *Pharm. Res.*, 2004, **21**, 1026–1033.
100 C. C. McLauchlan, G. R. Willsky, B. J. Peters and D. C. Crans, Vanadium-phosphatase complexes: Phosphatase inhibitors favor the trignonal bipyramidal transition state geometries, *Coord. Chem. Rev.*, 2015, 163–199.
101 D. Smith, P. Artursson, A. Avdeef, L. Di, G. F. Ecker, B. Faller, J. B. Houston, M. Kansy, E. H. Kerns, S. D. Krämer, H. Lennernäs, H. van de Waterbeemd, K. Sugano and B. Testa, Passive Lipoidal Diffusion and Carrier-Mediated Cell Uptake Are Both Important Mechanisms of Membrane Permeation in Drug Disposition, *Mol. Pharmaceutics*, 2014, **11**, 1727–1738.
102 D. C. Crans, L. Henry, G. Cardiff and B. I. Posner, Developing Vanadium as an Antidiabetic or Anticancer Drug: A Clinical and Historical Perspective, *Met. Ions Life Sci.*, 2019, **19**, 203.
103 T. Scior, J. Antonio Guevara-Garcia, Q.-T. Do, P. Bernard and S. Laufer, Why antidiabetic vanadium complexes are not in the pipeline of ''big pharma'' drug research? A Critical Review, *Curr. Med. Chem.*, 2016, **23**, 2874–2891.
104 C. Lipinski and A. Hopkins, Navigating chemical space for biology and medicine, *Nature*, 2004, **432**, 855.
105 C. A. Lipinski, L. Lombardo, B. W. Dominy and P. J. Feeney, Experimental and computational approaches to estimate solubility and permeability in drug discovery and development settings, *Adv. Drug Delivery Rev.*, 1997, **23**, 3–25.